PURDUE UNIVERSITY
GRADUATE SCHOOL
Thesis/Dissertation Acceptance

This is to certify that the thesis/dissertation prepared

By VARUN KUMAR KARINGULA

Entitled

MANUFACTURING PROCESS OF NANOFLUIDICS USING AFM PROBE

For the degree of Master of Science in Mechanical Engineering

Is approved by the final examining committee:

HAZIM EL-MOUNAYRI
Chair

LIKUN ZHU

RICARDO S. DECCA

To the best of my knowledge and as understood by the student in the Thesis/Dissertation Agreement, Publication Delay, and Certification Disclaimer (Graduate School Form 32), this thesis/dissertation adheres to the provisions of Purdue University's "Policy of Integrity in Research" and the use of copyright material.

Approved by Major Professor(s): HAZIM EL-MOUNAYRI

Approved by: SOHEL ANWAR 3/30/2015

Head of the Departmental Graduate Program Date

MANUFACTURING PROCESS OF NANOFLUIDICS USING AFM PROBE

A Thesis

Submitted to the Faculty

of

Purdue University

by

Varun Kumar Karingula

In Partial Fulfillment of the

Requirements for the Degree

of

Master of Science in Mechanical Engineering

May 2015

Purdue University

Indianapolis, Indiana

ACKNOWLEDGMENTS

First of all, I would like to express my sincere gratitude to my advisor, Professor Hazim El-Mounayri, for his guidance, encouragement and professional support during the thesis work. I heart fully appreciate him for believing in me and introducing me to this research area, which gave me lot of exposure.

I would also like to thank my committee members Dr. Likun Zhu and Dr. Decca for advising me throughout my research. Also I would like to extend my sincere thanks to Sudhir Shrestha, Mangilal Agarwal, and Jong Eun Ryu for providing me with their valuable advices in research.

I would also take this opportunity to thank Rapeepan, Birck nanotechnology staff for helping me in completing the thesis.

Finally, I would like to express my deepest appreciation to my mother for selfless love and support, and my friends and family members who supported me during this phase of my life.

TABLE OF CONTENTS

LIST OF TABLES

LIST OF FIGURES

Figure Page

Figure Page

ABSTRACT

Karingula, Varun Kumar. M.S.M.E., Purdue University, May 2015. Manufacturing Process of Nanofluidics Using AFM Probe. Major Professor: Hazim El-Mounayri.

A new process for fabricating a nanofluidic device that can be used in medical application is developed and demonstrated. Nano channels are fabricated using a nano tip in indentation mode on AFM (Atomic Force Microscopy). The nano channels are integrated between the micro channels and act as a filter to separate biomolecules. Nano channels of 4 to7 m in length, 80nm in width, and at varying depths from 100nm to 850 nm allow the resulting device to separate selected groups of lysosomes and other viruses. Sharply developed vertical micro channels are produced from a deep reaction ion etching followed by deposition of different materials, such as gold and polymers, on the top surface, allowing the study of alternative ways of manufacturing a nanofluidic device. PDMS (Polydimethylsiloxane) bonding is performed to close the top surface of the device. An experimental setup is used to test and validate the device by pouring fluid through the channels. A detailed cost evaluation is conducted to compare the economical merits of the proposed process. It is shown that there is a 47.7% manufacturing time savings and a 60.6% manufacturing cost savings.

1. INTRODUCTION

1.1 Background

Nanofluidics, as it applies to biochemistry, biophysics, membrane science, engineering and soil science, has become increasingly successful over the past decade [1] [2] [3] [4]. In fact, the range of applications of nanofluidics is broad. In 1965, Rice et al. found an equation through which they manipulated the flow by adjusting the sizes of pore radius and Debye length [5]. During the past few decades, there have been many developments leading to the development of technological tools, such as ion-beam lithography, the atomic force microscope, the scanning tunneling microscope, and a few other soft lithography techniques, all of which can create nano structures and allow researchers to conduct in-depth study regarding the properties of fluid passing through those channels. The above process and application of nanofluidics will be very useful in the future, as they will enable researchers to better address many questions that cannot be solved via microfluidics because of size constraints [6] [7] [8].

The movement to nanofluidics from microfluidics aims at better understanding the process at an atomic level, which grants the researchers the ability to address many unresolved problems. The solutions to some biological problems, such as biomolecule separation, cell communicators, and nucleic material filtration, can be studied by way of nanofluidics [2]. Microfluidics was a widely used technology during the 1980s because of its advanced features; it was able to reduce the size of the product, consume less of the testing units volume and energy, and use micro level domains. Initially, this technology was developed for use in inkjet print heads, Lab-on-a-chip, micro propulsion, and micro thermal technologies [9] [10]. While the use of microfluidics is applicable to a number of areas, it is really only effective for micro scale application. It is very important to know the science and engineering concepts of nanofluidics from

the atomic level, which provides researchers with ample motivation to develop a new time- and cost-efficient manufacturing process using tools that will have impact in the field of nanotechnology.

It is convenient to create nano channels that range from 10nm to1000nm using the existing techniques to create nano fabrication, but the key to developing the right process that will enable us to fabricate this advance manufacturing process is very important. Many biomolecules present in living beings fall under this category (10 to 1000 nm) [6] [11]. The goal of this research is to provide a better device to the medical industry.

1.2 Literature Review

Research and development in the field of a nanofluidics has led to many scientific discoveries in recent years. There are many different types of fabrication processes that allow for the development of new devices within the current industry. Researchers have used E-beam lithography to develop a nanofluidic device for bioanalytical applications such as fractionation, concentration, and separation. Research for the development of new technologies in biomolecule separation and biochemical transport in micro and nanofluidic devices has also progressed in the last decade.

The E-beam lithography process, widely used in developing nano fluidic devices, costs more, uses difficult, complex patterns, and is not suitable for large production in a limited time span. Cheng et al., fabrication process that has been proposed, nano-imprint lithography, uses E-beam lithography for nano scale features and optical lithography for large features, and requires a mold to be developed. The disadvantage to this process, however, is that we have to change the mold for each design. In this fabrication process, proposed by Cheng et al. [12], the hybrid PDMS-SI02 nanofluidic channels are fabricated. The Cheng et al., proposes a new etching process called electro chemical etching; this serves as an alternative process for removing material. In this process, the work piece is kept inside the electrolyte cell and used as an anode

while a salt solution is used as an electrolyte. When an electric current is passed through the electrolyte cell, the removal of material takes place. After the fabrication process, the work piece is bonded with the PDMS, which seals the device from the top. The device is then tested to see if there are any leakages.

Nano-channels were fabricated on silicon dioxide using a laser photolithography technique to fabricate a device for biomolecule separation. We also have a better chance of studying restriction mapping and fundamental polymer dynamics. The etching process was performed using HF. Wet etching was done on the work piece. The work piece was diced into small pieces, followed by anodic bonding to seal the upper surface. A DNA sample was taken and placed inside the nano slit through inlets. After the pressure at both ends were matched , DNA slowly started moving through the nano slit, which was observed by the fluorescence microscopy using 60XNA 1.3 immersion object. Madhavi Krishnan et al. [13], fabricated many variations of nano slits, and her experiment has introduced DNA samples into groups where the dimensions of nano channels are around 50 to 350 nm depth. It was observed that a group of DNA occupied near footprints of slits. Madhavi Krishnan et al., introduced DNA samples into nano channels whose dimensions were around below 100 nm. During this process, many extended DNA samples were breaking because of photo cleavage. According to the author slit depth and the Debye length influences the trapped molecule. There is a variation of frequency of current which is constantly passing through the nano slit. Recorded data can be used for further development of biomolecule studies.

Nanofluidic channels were fabricated on the borosilicate glass using the buffered oxide wet etching process. Glass-glass bonding is done in a furnace at 400°Cwith another flat cover slip. The depth of nanofluidic channel was about 40nm with an aspect ratio around 0.0002. Mainly for the applications such as proteins and biomolecule detection. This entire process was mainly concentrated on fabricating nano channels and doing the bonding in a less costly way. First, the mask was designed in AutoCAD software and was printed on a plastic sheet. The plastic mask now can be used for

pattern making. The channels are made parallel to each other, and the dimensions are 40mm long and width spaced 500m from each other. Capillary action introduces the fluid inside the nanofluidic channel due to large surface to volume ratio. To evaluate the hydrophilic nature of glass, the contact angle is measured first, and it is reduced by cleaning the glass with piranha solution. After that, the substrate was dipped in 1 M HCI solution for 2 minutes to remove the additional dust particles. Nanofluidic channels, which are 40 nm deep, are filled with DI water without any external driving force. The results are useful for nano-fabrication and for ultra-sensitive detection systems in the next generation of nanofluidic device application [14].

Zhi-Qian et al. [15], describes a feasibility study of realizing nano channels only on hard silicon oxide layer using AFM-based nanolithography. The fabricated nano channels can serve as a platform for achieving a single biomolecule analysis in a nano fluidic system. As done for the first AFM lithography method, Zhi-Qian et al., collected the data achieved after doing the second AFM lithography method, which the mean depth, maximum depth, peak depth and their relationship with the applied cutting stresses are computed. The average depth of the nano channels machined on the silicon oxide surface using first AFM lithography technique at cutting force = 6.8 N, 10.8 N, 2.8 N, and 14.8 N are 6.5 nm, 13.1 nm,14.6 nm, and 12.7 nm. The maximum depths achieved are 12.9 nm, 23.1 nm, 28.2 nm, 21.2 nm respectively. The limitation in their study was that they tried only on one material to determine the properties of silicon oxide.

A process of soft photolithography was proposed by Cao and Yu [16] to fabricate 10 nm enclosed nano fluidic channels. NIL was used to fabricate the nano channels. The mold was generated by interferometric lithography and has 200nm period gratings over a 100 mm diameter wafer. Nano channels on the mold developed by interferometric lithography were limited by the wavelength of the light used for exposure, about 100nm. To close these channels, sputtering was performed and was followed by anodic bonding.

Recently, nanofluidic channels have been used to better understand the transportation phenomena of nano particles inside the fluid. Kemery et al. [17], found that by combining the two dimension parameters, which are channel diameter a and inverse Debye length K, we will be able to control the flow in processes such as electro-osmosis and electro-migration. Controlled flow can be possible when we change EDL thickness with respect to the diameter of pore. This will significantly alter the concentration of electrolyte solution or influence the charge.

With the work contributed by the researchers in the field of nano flows, intermolecular forces, and surface forces there is a possibility of calculating factors such as ion-ion synergy, which is the amount of hydration caused in the nano spaces because of the fluid [18] [19] [20]. The change in length can also impact separation and study of biomolecules such as DNA, RNA, and others in nano dimensions. Research conducted by Petersen et al. discussed this subject in depth [21]. Immense growth of microfluidics in the semi-conductor industry has led to the development of a field that was unable to fit using microfluidics. Prakash et al [22], found that integrating nanofluidics systems in complex matter transportation systems can solve many problems of molecular gates and fluidic architecture, which are similar to very large scale integrations.

Nanofluidics plays a key role in chemical analysis and uses its functions to manipulate the analytical chemistry. The major applications of nanofluidics will be useful in producing effective injections and identification of chemical components that can measure quality and the quantity. Cannon et al. found that NCAM functions do have controllable gates that can transfer the amount of fluid r from one micro channel to another micro channel and also can be monitored by a graphically represented chart in the system that shows the fluid characteristics. Nanofluidics also has a very important role in novel separation of any sample. The principle behind this has been briefly explained by N.Laachi et al [23]. Nano fluidics will help in magnifying the image of the chemical and helping researchers understand the chemical in detail. The same principle is used in DNA separation in bio-medical applications.

In addition to the above applications, nanofluidics also has a huge impact on fields such as nano medicine and water purification. For several decades, nanofluidics has been at the forefront of developing some extraordinary technologies to change the process rapidly and generate faster, more precise results. Raw material waste is reduced as well. Freitas et al. [24], briefly explain the concepts of nano medicine as well as the advancements achieved by researchers in that particular field. Presently, silicon is extensively used in making micro devices because of its extraordinary qualities, but researchers are always looking for other materials to make more efficient nano devices. Tung et al. [25], developed a sensor in which bacteria acted as motors in pumping a small amount of liquid. Because of increase of pollutants worldwide, water is frequently becoming contaminated. The level of contamination has been reported in many international surveys [26] [27]. Nano structures such as nano pores or nano channels of width will play a crucial role in purifying contaminated water. A study conducted by Gardeniers et al. on the analysis of small particles explains the importance of using such devices in the future. The integration of nano structures in micro level devices can be effective and can produce some extraordinary results.

1.3 Thesis Objective

Previous techniques used to manufacture nano channels have been unique, but most of them used e-beam lithography to generate nano channel fairly used for development on nano-channels for research purposes. This particular way of manufacturing is expensive and leaves little room for flexibility, which is necessary, as new mask should be designed for each variation implemented in the nano-channel. Followed by expensive etching process to create channels which is done in the clean room. Additionally, one issue with e-beam lithography is that when we change the base material, the energy of ejecting electrons needs to be adjusted, and this results in time spent developing formulas for different materials.

The purpose of this thesis is to carefully develop a manufacturing process for nanofluidics that is much more cost-efficient and which gives us more flexibility to vary the size and shape of the nano channel at any given time while developing the device. We will be using an atomic force microscope to generate nano channels using indentation mode. There are many advantages to implementing this manufacturing techniques; these include the use of fewer chemicals, greater efficiency regarding both time and cost, avoidance of harmful radiation, as well as etching and fabricating the nano channels. This flexibility allows for change in dimensions, ability to generate 3D images parallel while fabricating the nano-channels, and opportunity to study the materials on which the nano channels are being created. This process is affordable to students and researchers who would like to further investigate the application of nanofluidics on a low budget. The innovative manufacturing process of nanofluidics for medical application is discussed in detail in upcoming chapters.

1.4 Thesis Outline

This thesis includes detailed descriptions of previous works and applications of devices in various emerging fields. Further reduced cost fabrication processes are studied and utilized in our fabrication process. The fabrication of micro channels is described in detail in Chapter 2, and key points, such as photo-mask design, the photo-lithography process, dry etching are described. In Chapter 3, fabrication with indentation mode using atomic force microscopy is performed and discussed. PDMS mask is used to seal the top surface of silicon, and it is one of the most cost-efficient ways to close the top layer, and validation testing will be performed to see the effective bonding between the silicon and PDMS mask this technique is clearly discussed in Chapter 4. Detailed discussion of results will be in Chapter 5. Chapter 6 provides a detailed summary and conclusion.

2. FABRICATION OF MICRO CHANNELS

2.1 Overview

Photolithography is one of the most widely used fabrication process for building microfluidic channels. In this chapter, fabrication of the microfluidic channels on the top of silicon wafer using the photolithography process is explained in detail. In our application, these fabricated micro channels will serve the medium as inlet and outlet for our nano channels. Silicon is the most popular material in building micro and nano devices because of its unique qualities. Design of these microfluidic channels were made with smooth finish surfaces by keeping in mind the flow of fluid which passes through these channels. Spacing between the sets of micro channels were placed at different lengths to study our device in the most efficient way, which was clearly shown in the mask. The implemented fabrication process was straightforward and has been used by many researchers in various applications [28] [29] [30].

2.2 Fabrication of Micro Channels on Silicon Wafer

The fabrication process was performed in a "Class 100" cleanroom at BIRCK Nanotechnology Center of Purdue University. The clean room can be defined as a room with a very low level of environmental pollutants and is used for scientific research in fabrication of micro and nano level devices. The clean room can be classified into the quantity of particles permitted per volume of air. The below Figure 2.2 clearly shows the types of cleanroom according to their allowances of dust particles. There are certain steps to follow while performing photolithography process, and these are discussed in the upcoming sub-chapters.

The dust particles are identified by a light scattering instrument, which is useful in determining the sizes and quantity of small dust particles.

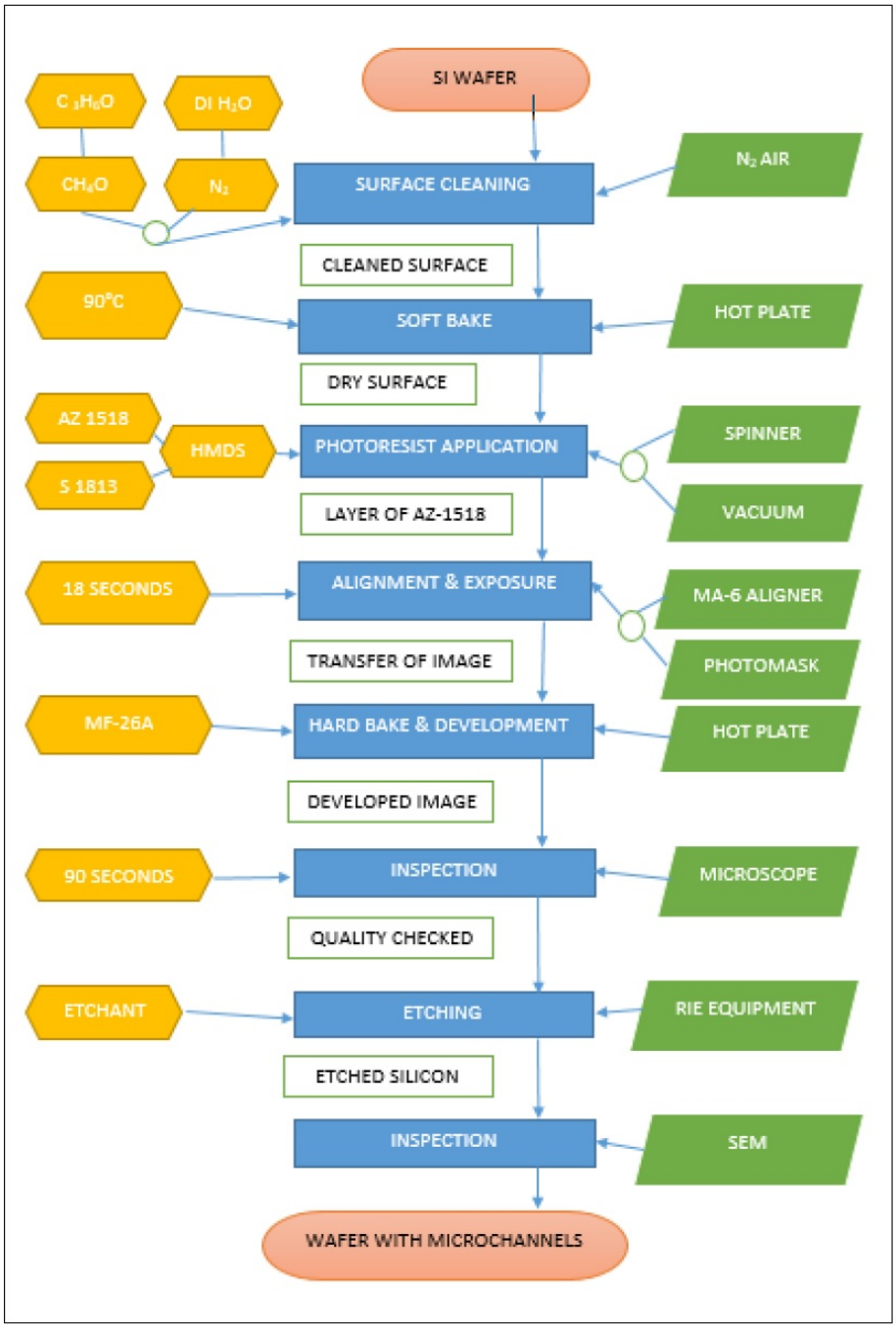

Figure 2.1. Process flow during the fabrication of micro channels

2.2.1 Surface Cleaning

Silicon wafers are used as the raw materials to build this device because of their unique properties. This process was conducted at advanced nafer.no fabrication lab

US FED STD 209E cleanroom standards

Class	maximum particles/ft^3					ISO
	≥0.1 µm	≥0.2 µm	≥0.3 µm	≥0.5 µm	≥5 µm	equivalent
1	35	7.5	3	1	0.007	ISO 3
10	350	75	30	10	0.07	ISO 4
100	3,500	750	300	100	0.7	ISO 5
1,000	35,000	7,500	3000	1,000	7	ISO 6
10,000	350,000	75,000	30,000	10,000	70	ISO 7
100,000	3.5×10^6	750,000	300,000	100,000	700	ISO 8

Figure 2.2. Standards of clean rooms [31]

at BIRCK nanotechnology center at Purdue University. To clean the silicon wafer, we performed a surface preparation operation to remove the maximum dust particles from the top of the wafer. There may be many different kinds of dust particles that have accumulated on the top of the wafer, such as dust from scribing or cleaving, atmospheric dust, abrasive particles, lint from wipers, photoresist residue from previous photolithography, and bacteria. We first rinsed the wafer with DI water for 5 minutes. Then, we rinsed the wafer with acetone and again with DI water. Finally, the wafer was exposed to dry nitrogen to clean the moisture from it. This process removes the dust particles that had been deposited on the top of the wafer.

2.2.2 Soft Bake

Soft bake operation is performed on the top of the wafer on which the photoresist has been deposited. This operation will improve adhesion, uniformity, and linewidth control, and it also optimizes light absorbance characteristics on top of the photoresist. The wafer is baked in the oven for 90 degrees for 2 minutes; this pre-bake operation removes humidity that had been deposited on top of the wafer.

Table 2.1. Process of surface cleaning

STEPS	PROCESS
1	Soak the wafer in the acetone solution (C_3H_6O) for 2-5 minutes
2	Soak the wafer in methanol (CH_4O) for 2-5 minutes
3	Soak the wafer in DI water (DI H_2O) for 2-5 minutes
4	Rinse with free flowing water for 30 seconds
5	Expose the wafer with dry nitrogen(N_2); blow until there is no moisture

Table 2.2. Process for soft bake

Temperature	Time
90	120

2.2.3 Photoresist Application

Before applying the photoresist on top of the silicon wafer, we use primer on the top of wafer and rotate with the formula in two steps. The first step runs on 500 rpm for 5 seconds, and the second step runs on the speed of 3500 rpm for 40 seconds; this will ensure uniform distribution on the top surface.

Next, a positive photo is used in this fabrication process. Primer will help photoresist to distribute on the top layer without many air bubbles. We use the same formula for spinning, which is 500 rpm for 15 seconds and then 3500 rpm for 45 seconds.

Photoresist thickens on the top of the wafer depending on factors such as spin speed, solution concentration, and molecular weight.

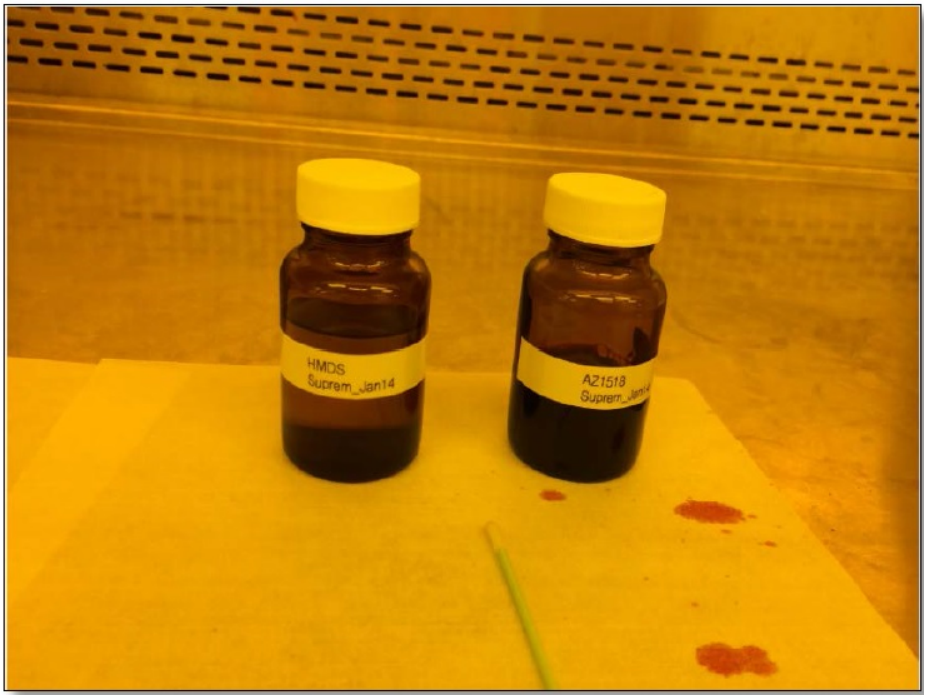

Figure 2.3. Bottles filled with AZ-1518 and HMDS

Table 2.3. Raw materials used in photoresist application

Primer	Hexamethyldisilazane (HMDS)
Photoresist	AZ-1518

Table 2.4. Operations implemented in photoresist application

STEP (S.no)	TIME (seconds)	SPEED (rotations per minute)
1	5	500
2	3	500-3500 (ramp)
3	40	3500

2.2.4 Alignment and Exposure

To perform align and exposure operation, we used the facility at BIRCK Nano technology center at Purdue University. The MA6 aligner is utilized to perform very

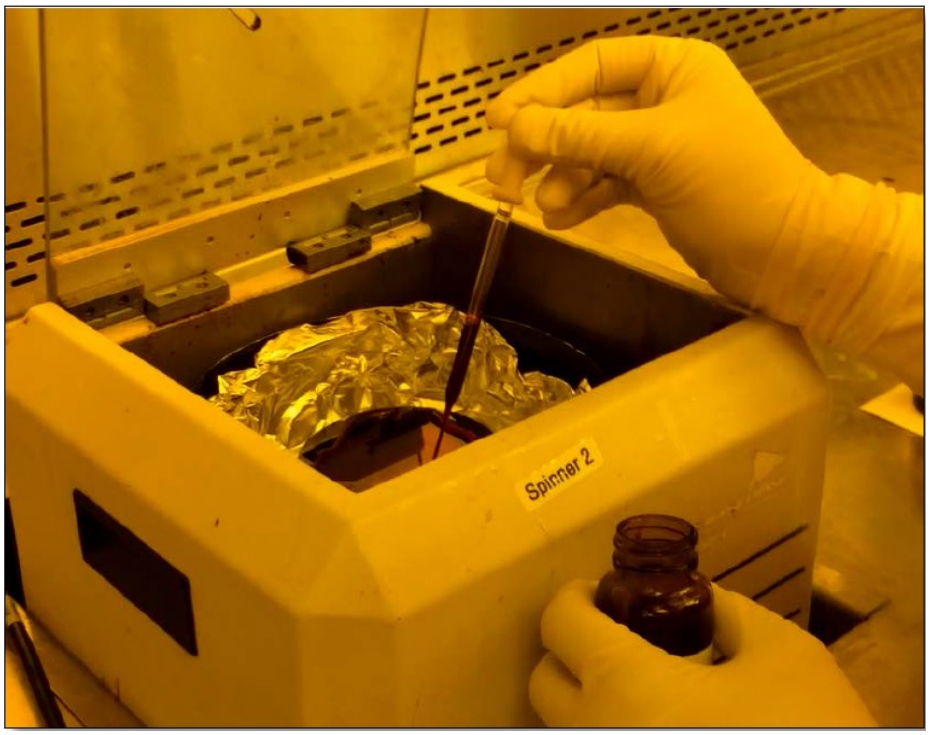

Figure 2.4. Photoresist application

advanced exposure. MA6 aligner has optical contact of ratio 1:1 because of which when the source exposes ultraviolet light the image is transferred from mask to the wafer. The set point of the MA6 aligner is 405 nm. The 5 inch mask was specifically created for performing this operation as MA6 aligner. The mask was exposed on the top of the silicon wafer for 18 seconds at the intensity of ultraviolet radiation. The purpose of this exposure system is to deliver light to the wafer with proper intensity, directionality, spectral characteristics, and uniformity.

The MA-6 aligner is used for mask alignment with the wafer; the instrument uses ultraviolet radiation for imprinting the mask on the top of the silicon wafer. The MA6 aligner has an option of storing the recipes, and the internal memory allows users to save their data and to access that data at any time.

Where 'R' is resolution of image, 'λ' is wave length of light, 'z' is photoresist thickness, 'NA' numerical aperture, and 's' is spacing between substrate and mask.

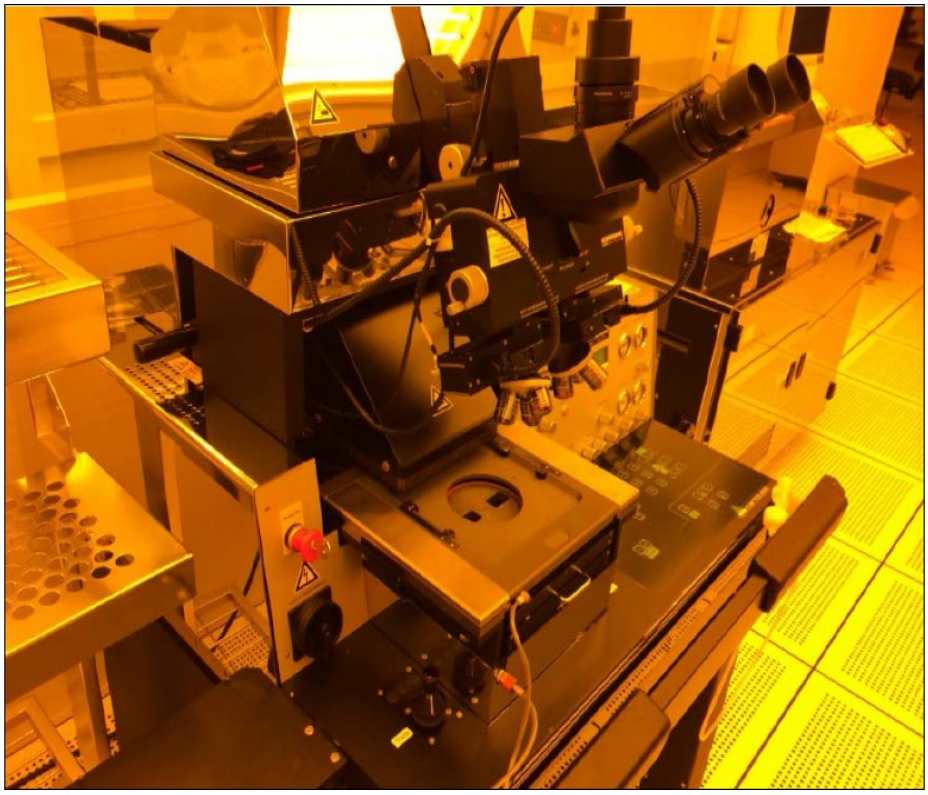

Figure 2.5. MA-6 aligner used as ultraviolet light source

Contact	Proximity	Projection
$R = 2b_{min} \approx 3\sqrt{\lambda \frac{z}{2}})$	$R = 2b_{min} \approx 3\sqrt{\lambda s}$	$R = 2b_{min} = 0.6\ \lambda/NA$

Figure 2.6. Resolution of image during different modes [32]

2.2.5 Hard Bake and Development

To develop the pattern which was imprinted on the top of the silicon wafer, we have utilized an MF-26 developer. The wafer has been subjected to total immersion inside the developer for 60 seconds, which will remove the photoresist and develop the micro channel pattern on the top of the wafer. Constant movement of the wafer inside the solution will ensure the complete removal of photoresist.

Table 2.5. Represents Operations execute

Operation	Specifications
Thickness Photoresist	2 microns
Intensity of light	14 mW/cm^2
wavelength	450 Nm
exposed time	18 seconds

2.2.6 Inspection

After developing the micro channels on the layer of photoresist, the next step of inspection is to check the quality of micro structures formed on the top of the photoresist during the process of photolithography. As there is continued possibility of shrinking on the micro channels, a more advanced inspection process is necessary.

An advanced mechanism optical microscope is used for checking the image of the micro structures manually. The formation of critical dimensions is very important for the improved performance of a device, and optical scales are present in the microscope, allowing us to measure the dimensions of the device.

There are two inspections done, one after development process to check the micro structures transferred from mask to wafer with top layer of photoresist and another after the etching process, where silicon material is removed during the RIE process. The level of etching process can be evaluated by checking the microstructures through SEM. Key factors such as channel depth and space between two channels are measured during this process.

2.2.7 Etching

In this particular process, reaction ion etching has been performed on the top of the wafer. Dry etching removes the material from the top of the silicon and

uses high reactive plasma. Low or high density plasma can be generated under low pressure under electromagnetic field and also produces a clean process, compatible with automation, anisotropic etching, and precise patterns, especially for nano-scale features.

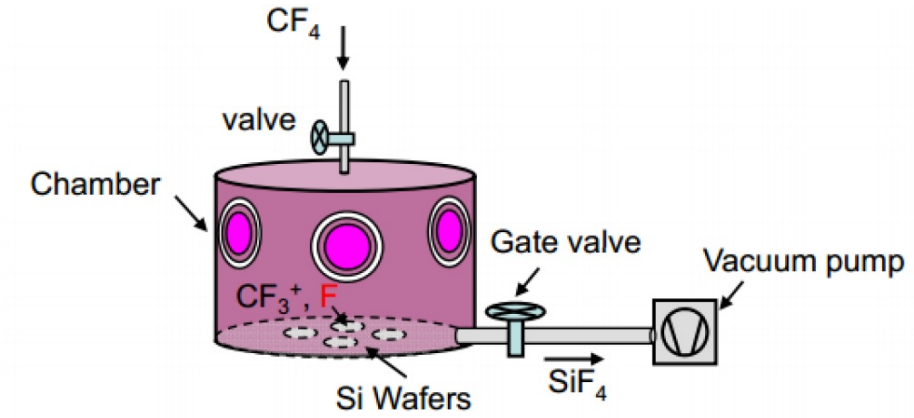

Figure 2.7. Plasma vacuum system [33]

Capacitive RIE Low density plasma N=$10^9[electron/cm^3]$; ionization efficiency=10^{-7}; Inductive RIE' High density plasma .N=$10^{13}[electron/cm^3]$; ionization efficiency =10^{-3}.

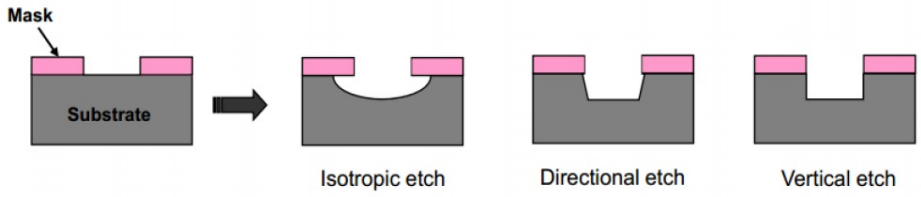

Figure 2.8. Variation of material removal with different types of etching processes on sample [33]

Reaction ion etching is done in the presence of high density plasma, which produces lower ion bombardment energies, as shown in Figure 2.8.

Lower ion energies will result in lower etch rates and reduced anisotropy. The etch rate can controlled depending on the density of plasma; when operated under low pressure, the anisotropy can be controlled. Radicals and ions play very important

Table 2.6. Process of reaction ion etching

	SWITCHING TIME	PRESSURE	RECOIL-POWER	RE BIAS POWER	GAS FLOW [SCCM]
ETCH	8.5 SECONDS	40M TORR	2200W	40 W	40 W
PASSIVATION	3 SECONDS	14M TORR	1500W	20 W	20 W

roles inside the reaction ion etching. Positive ions are essential for the smooth etching process. Radicals have a longer lifetime compared to ions. When ions collide with the surface, ions becomes neutralized, but in the case of the radicals, they do not react. Instead, they reflect back into plasma.

3. FABRICATION OF NANO CHANNELS

3.1 Nano Fabrication Overview

It can be defined as the study of fabrication process for creating nano meter scale structures. This technology is used for a variety of applications in the semi-conductor industry and nanoelectromechanical systems. Fabrication of nanostructures can be done by two approaches: top down approach and bottom up approach. When the nano-channel is created on the top of the material, it is considered to a top-down approach. The other approach which involves creating the nano structures involving interaction of molecules or colloidal particles can be considered a bottom-up approach. Photolithography, x-ray lithography, double patterning, electron-beam lithography, and ion beam lithography are the few examples of bottom-down approaches. There is a very high cost associated with fabrication of nanostructures with bottom-up approach which are generally used in semi-conductor industry. In the last decade, several new methods have been developed that can fabricate nano channels on top of the substrate with much less expense. One top-down approach that is cost-efficient for performing fabrication of nanostructures is Atomic Force Microscope (AFM)-based nanolithography. The implemented fabrication process was straightforward and was successfully performed in various different applications [15] [34].

3.1.1 Atomic Force Microscopy

After its invention in 1986 by Binning, Quate, and Gerber [35], atomic force microscopy was majorly used to study the topography of the surfaces at atomic resolution. The Atomic force microscope can capture the images of resolution up to 10-10 m. There are large variety of materials with which images can be obtained.

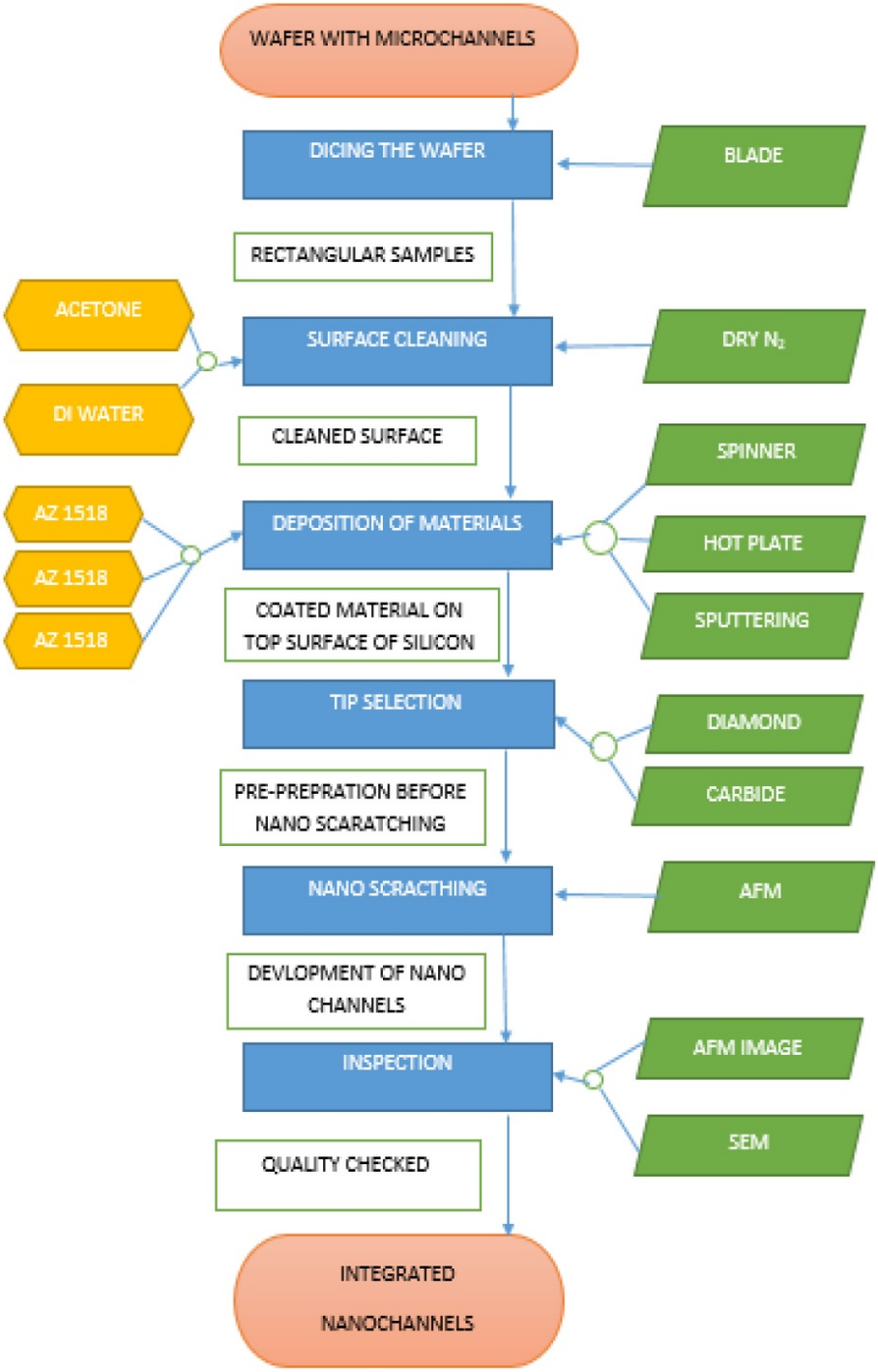

Figure 3.1. Process flow for fabrication of nano channels

The main principle on which the atomic force microscope runs is that when the tip, which is integrated at end of cantilever, is brought very close up to interatomic distance of the sample, there is a potential developed in the interatomic level. This generated force makes the cantilever deflect in the y-axis. The deflection of the cantilever is immediately captured and subjected to mapping by the laser detector.

A brief explanation of the principle can be observed from the following Figure 3.2. In this current Figure 3.2, the tip of the atomic force microscope is at an interatomic distance from the sample, which results in deflection in the cantilever. The force at the atomic level is measured by laser detector. The laser emits the light constantly on the top of the cantilever beam. Any deflection will be immediately captured by laser detector and shown on the computer screen, which will have a relative formula to determine the atomic force. The special feature about AFM is it can capture three-dimensional images, when the sample holder moves close to the tip using piezoelectric scanning tube. If there is any movement along the Z direction, it can be recorded. The atomic force microscope is used in various industries to determine the rigidity of materials in atomic scale.

3.1.2 Contact Mode

In this mode, the tip is in contact with the sample. When the scanning starts, a constant cantilever bend is maintained. If the tip is subjected to any intra-atomic force from the sample, then cantilever deflects more in the Z axis (zt), and it can be recorded on the monitor. The motion Z scanner is directly dependent on the sample topography and varies accordingly. One challenge users might face in the study of the topography of different materials is contamination on the top of the surface. Any hard dust particle on the top of the sample might cause damage to the tip when it is working on contact mode. Also, when the tip comes across the small contact surfaces, there is always a possibility of developing high contact surfaces that may result in breaking the tip or sample [36].

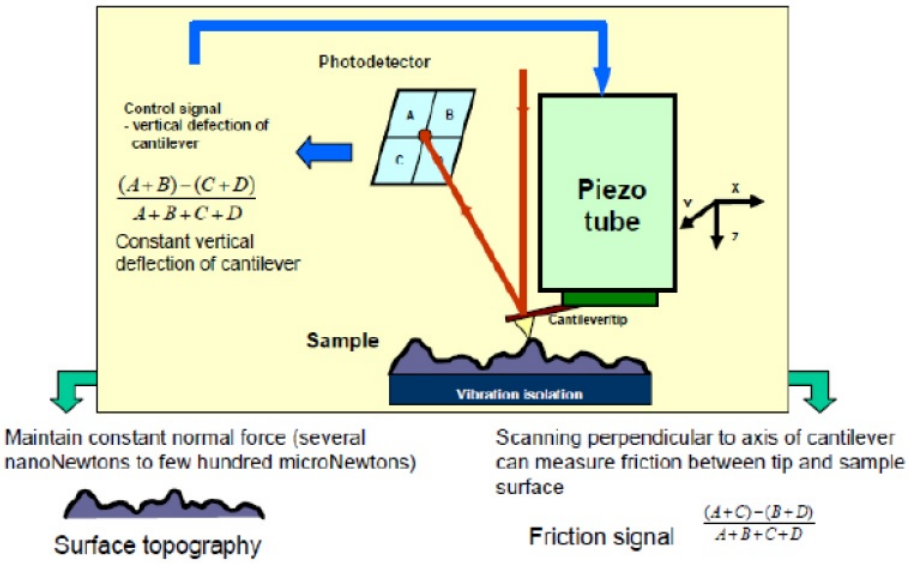

Figure 3.2. Contact mode of AFM

3.2 Pre-Preparation Before Nano Scratching

To use the atomic force microscopy for fabricating the nano channels, the sample should be small. As shown in the Figure 3.4 the atomic force microscopy holder can only accommodate a particular size with which the tip can indent inside the silicon material and perform nano scratching. An electronic wafer cutter has been used to cut the 4 inch wafer into pieces as shown in Figure 3.3. Before performing this operation, the photoresist layer is coated on the top of the silicon wafer to avoid dust particles from depositing in middle of the micro channels during the cutting. To remove the photoresist layer from the top of the silicon wafer, the surface cleaning operation is done using acetone as and DI water.

Acetone will erase photo resist and other dust particles, and moisture can be removed by using dry nitrogen.

To study the nano scratching on different materials, we deposited different top layers such as gold and photoresist S 1813 on top of the silicon wafer photoresist. This process will not only help studying the nano scratching on the top of different

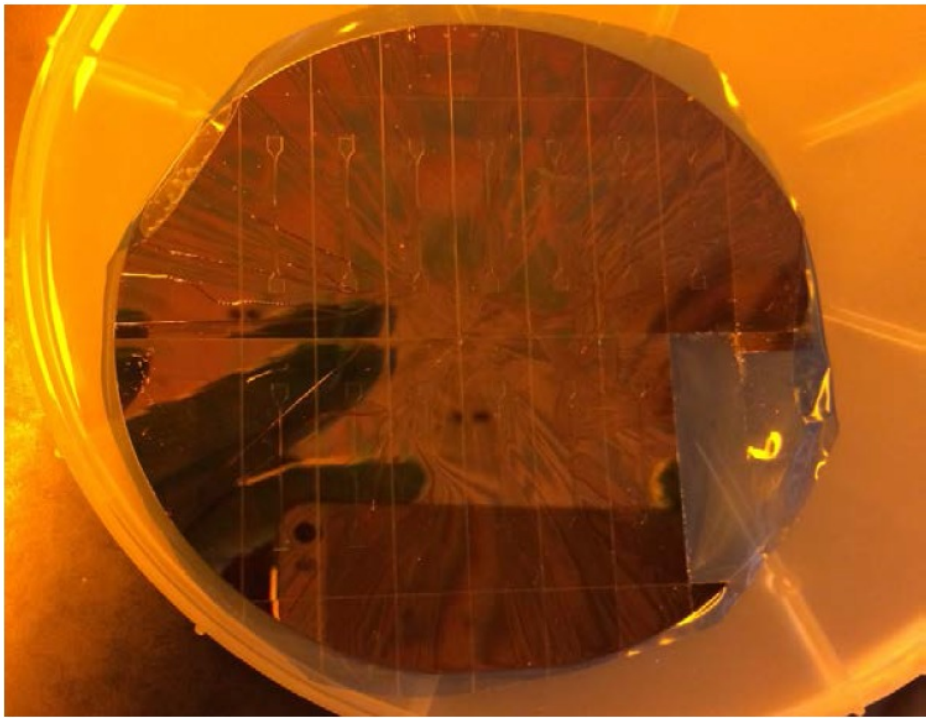

Figure 3.3. Silicon wafer diced with electronic blade

materials, but it also helps determine the most cost-efficient process to be affordable for medical uses.

To deposit 200 nm of gold on the top of the silicon micro channels, we used gold sputtering equipment. During the process, a hard gold sample is subjected to change its state into plasma.

This phenomenon happens when the blower takes all the air out and creates a vacuum in the chamber. The DC current is maintained at 28 m amps, and the rate of deposition is around 9 nm for every 30 seconds of time. The Figure 3.5 displays the equipment which was used for depositing the gold layer on the top of silicon surface.

3.3 Materials and Methods

The tip used in atomic force microscope is made up of tungsten-carbide [37], shape of the probe is hemispherical cone. The length of this particular probe is 225 um,

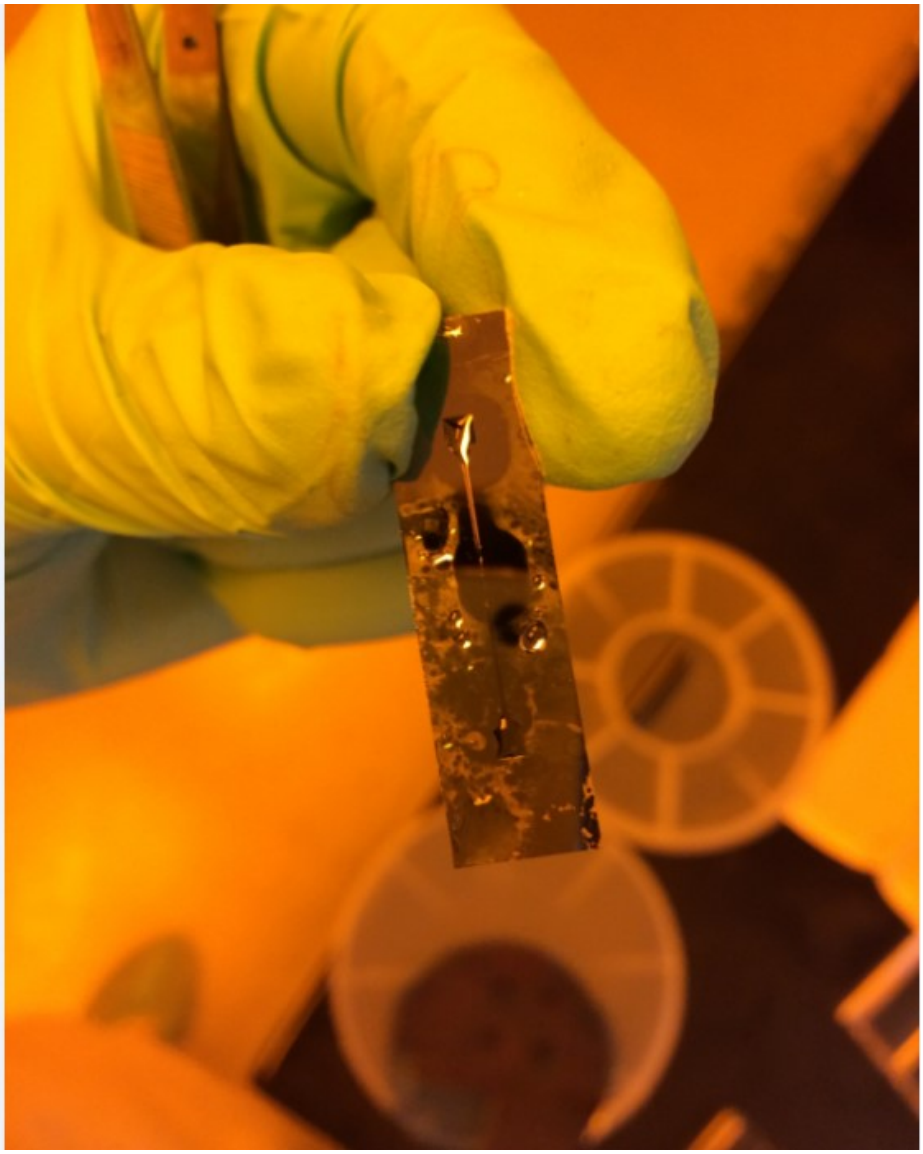

Figure 3.4. Diced wafer of 1.5 X 0.375 inches

spring constant is 3.0 N/m, and resonating frequency is around 75 KHZ. The material of cantilever is silicon of width 35 um. The tip radius is around <60 nm. Another tip which is used for the indentation is a diamond tip [38]. Generally, diamond tips are very expensive when compared with silicon tips because the fabrication is expensive. The tip is designed to provide ultra-high strength to the probe. When probe material

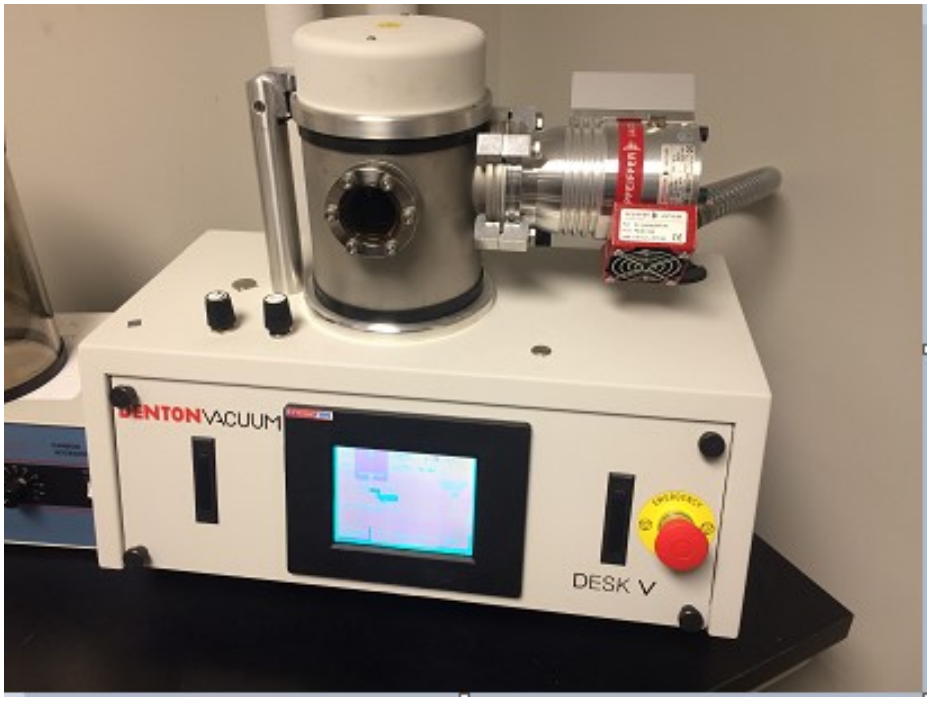

Figure 3.5. Denton vacuum used for gold deposition

is not harder compared with the substrate material, it tends to break as soon as it gets in contact with the top surface.

Using the diamond tip will be a clear advantage strength-wise compared to the other tips. These kinds of tips are not used for imaging purposes, but they are used to perform indentation modes on the materials. They are recommended to use only in air but not in liquids due to contamination issues. The cantilever on this probe is made of stainless steel in a rectangular shape, the length is around 11-15 um, and the thickness is around 13 um. The tip height is 50 um, normal tip radius is 40 nm, and maximum tip radius is 50 nm.

To create the nano channels on the top of the silicon substrate, we used a Veeco Bioscope Atomic Force Microscopy. A diamond probe along with a spring constant of 250 N/m was used in the experiments. The tip is of a pyramid shape, and the sharp edge is pointed downwards towards the sample. The tip will be intended inside the sample and will scratch the surface with the desired aspect ratio.

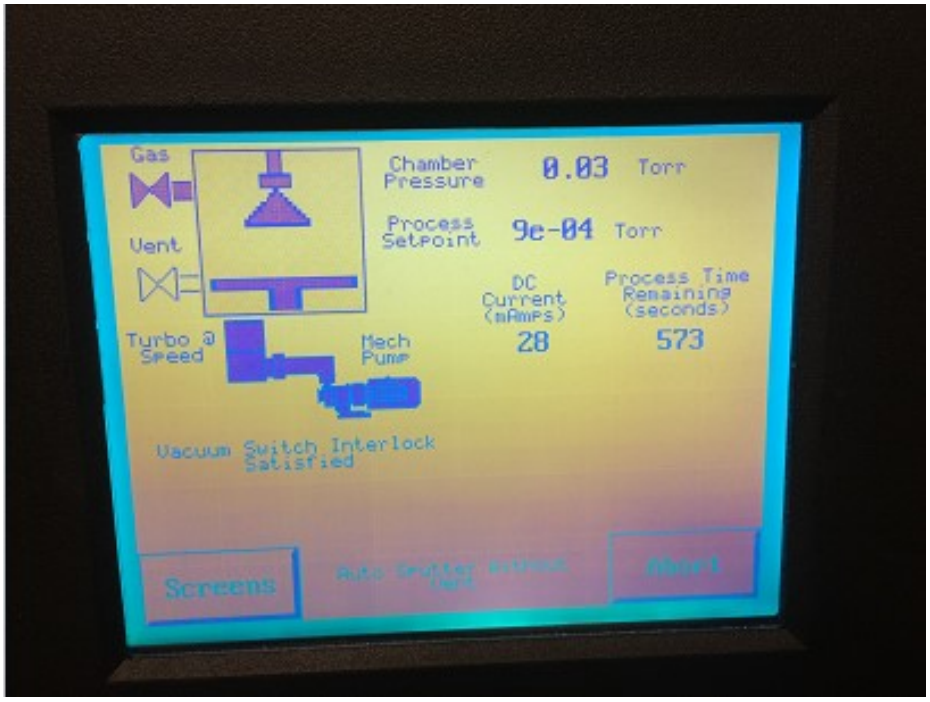

Figure 3.6. Pressure and DC current inside the chamber

The durability of tip was tested by performing the indentation mode on the top of the gold sample. Different forces were applied on the tip until the required deflection was achieved on the cantilever. The tip was moved in a horizontal direction until reaching the desired length, and then it was slowly lifted upwards to the initial position. Atomic Force Microscopy can be used to make anno channels of desired length, width, and depth according to our application. The advantage can be the 3D images which provide a much clearer understanding of the materials at the nano scale.

These nano channels were made out of scratching in indentation mode in the atomic force microscope. We tried to study different materials such as silicon, gold, polymer AZ-1518, and polymer S-1813 to try different manufacturing techniques which can be most efficient. The diamond tip is used to scratch the surface on the top of the silicon wafer. Diamond is stronger than any other material, and these specific tips were made thicker, wider, and longer for the efficient functionality. The range of spring constant for cantilever beams, which hold these types of tips around

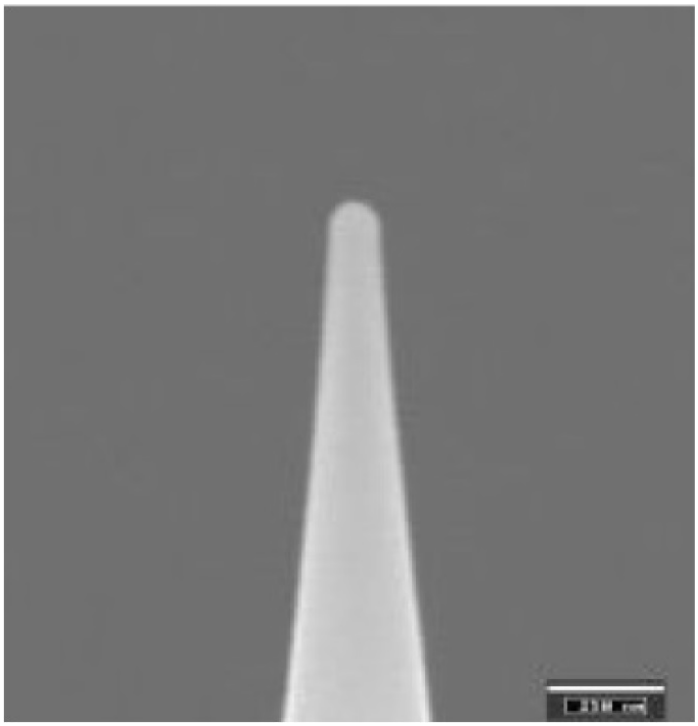

Figure 3.7. Image of AFM silicon carbide tip [39]

0.01-1.0 N/m, and the resonating frequency will be around 35-70 KHz. The diamond tip used for scratching also can be used for taking clear images.

Nano scratching on the gold, polymer AZ-1518, and polymer S-1813 was made using BioScope Catalyst. The tip used for making the AFM was made out a silicon cantilever coated with a carbide tip. When compared with the surface of silicon, these materials are softer and can be easily indented with the silicon carbide tip. These tips were used to make the manufacturing process of nano channels.

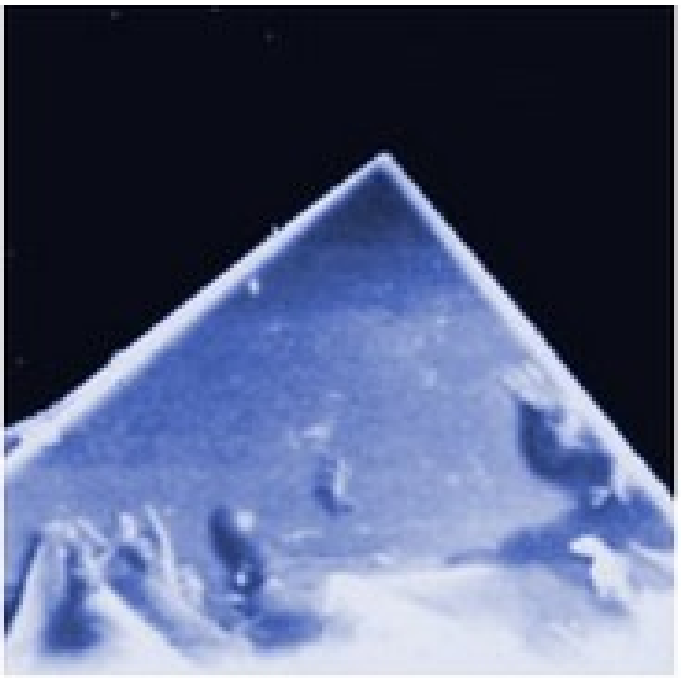

Figure 3.8. Image of diamond tip [39]

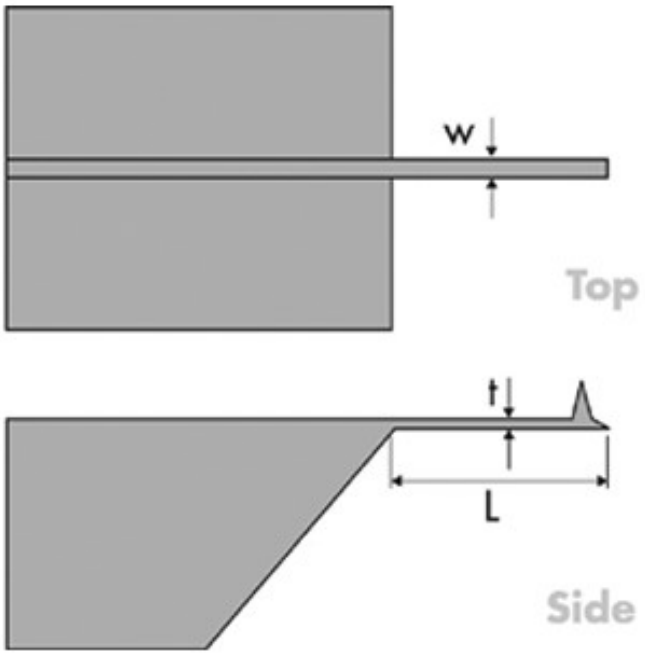

Figure 3.9. Side view of AFM diamond tip [39]

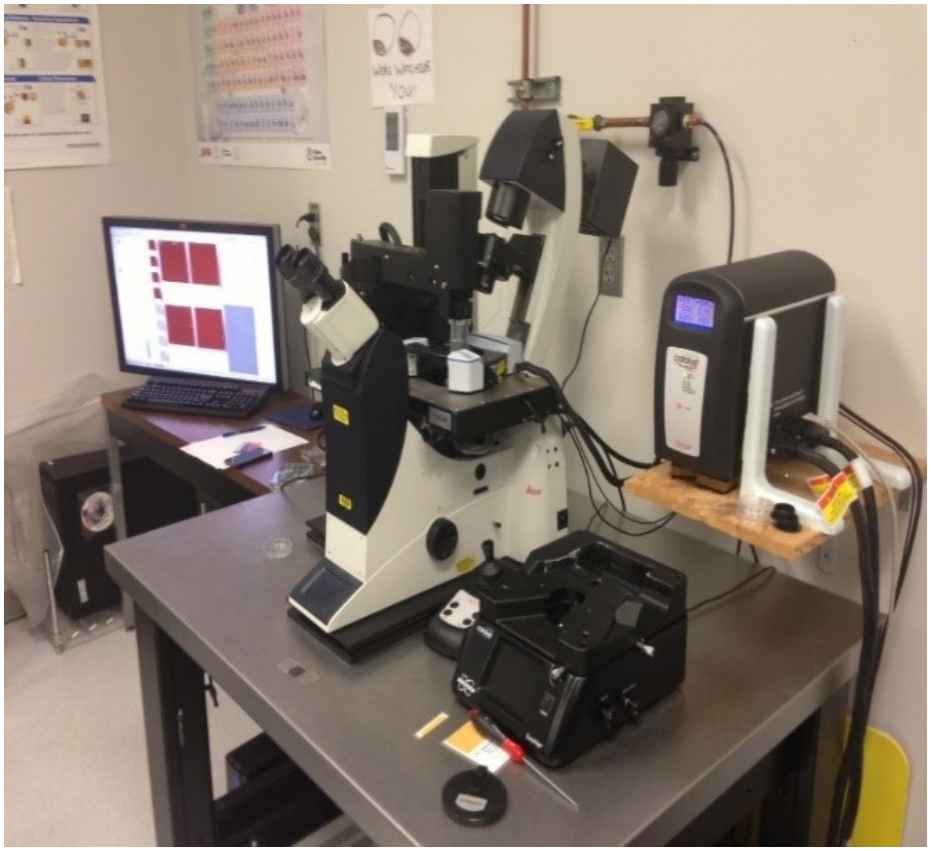

Figure 3.10. Bioscope Catalyst

4. FABRICATION OF SEALING PROCESS

4.1 Overview

There are many different bonding techniques which are generally used to seal the two materials. In the semi-conductor industry, the two techniques most frequently used to seal the materials are anodic bonding and PDMS bonding. There are multiple factors to consider when selecting a bond technique depending upon application. In this chapter, we will be discussing these two bonding techniques in detail.

Anodic bonding is one of the most common bonding techniques used to seal the micro and nano channels. This bonding technique was first reported in 1969. Previously, many researchers utilized this technique to seal the two materials for MEMS and other sealing applications [38] [40]. Yu-Qun et al. [41], conducted research to study some of the mechanical behavior of internal layers of Pyrex glass, silicon, and aluminum. They found that bonding tensile strength increases with the increase in temperature and voltage. On the other end, the bond tensile strength with the decreased AL intermediate layer because the formation of the nano layer in between will help form new bonds, resulting in more strength. Lee et al. [42], has presented a paper about the parameters that influence the bond time, such as magnitude of force, applied voltage, and surface cleaning. He tried three different type of cleaning by changing the chemicals and the voltage. Lee et al., also developed a graph between the bond time vs applied voltage and concluded that voltage will have a huge impact on the time of bond formation.

To check the effectiveness of temperature influence in the bonding, Wei et al [44]., conducted anodic bonding with a low temperature to study the strength of bond. They used a silicon wafer and a glass wafer (Pyrex 7740) to develop anodic bond between them. To check the tensile strength of the bond, they used the Taguchi

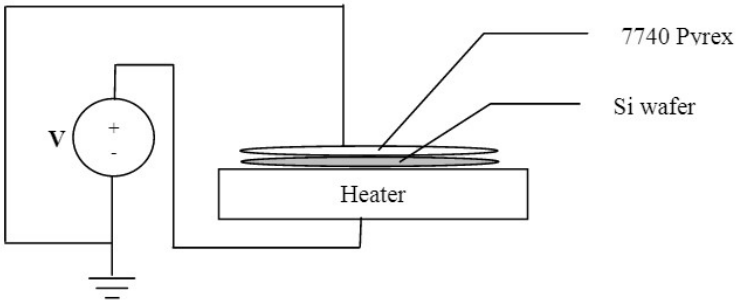

Figure 4.1. Generic anodic bonding setup [43]

method. They found that the bond strength is higher than 10 MPa and increases by varying the temperature. Sometimes very high temperatures can also be the reason to self-develop the cracks in the glass during the bonding. Cho et al. [45], analyzed improving the anodic bonding strength by pre-treating the silicon and glass wafer with oxygen plasma.

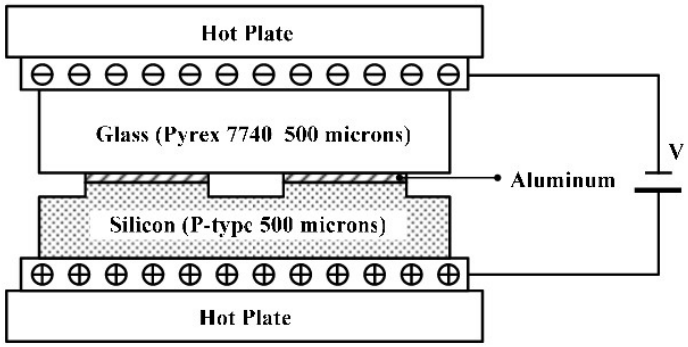

Figure 4.2. Bonding of positive and negative ions of Pyrex and silicon [41]

Cho et al., has performed experiments by treating the two wafers of silicon and glass with oxygen plasma and has performed the anodic bonding with a low temperature. The results show that the oxygen plasma treatment has a significant impact on the bonding process. The oxygen plasma treatment reduced the contamination with

which bond strength and other electrical properties increased. Also, oxygen plasma has induced high polar and low dispersion characteristics, ultimately increasing the surface energy.

When the concentration of plasma power and exposure time increases, the surface roughness also increases, causing better bonding between the surfaces of silicon and glass.

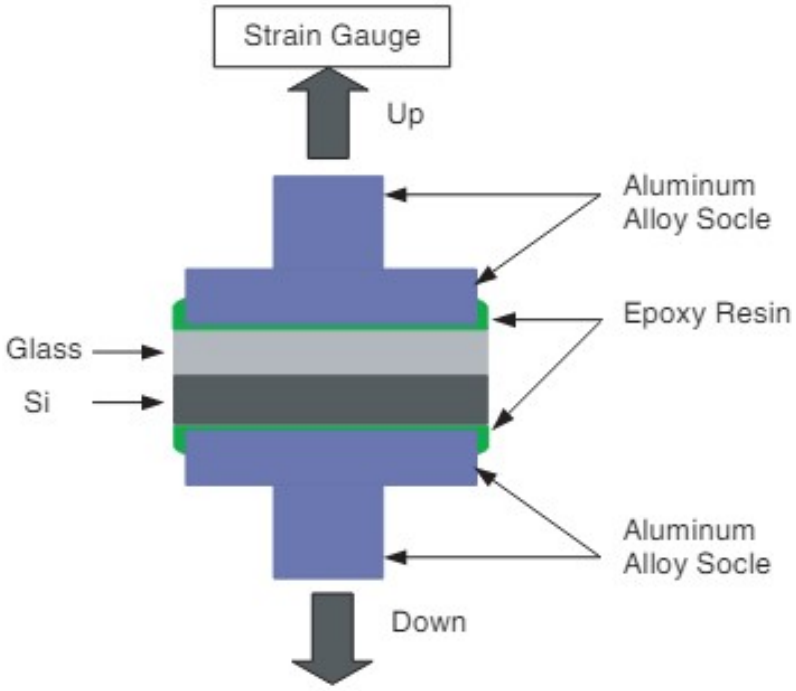

Figure 4.3. Validation testing to determine the bonding strength [44]

Conventionally, researchers were using the anodic bonding in the 1990s. Although there were many advantages by using the above process, there were also disadvantages. Because of these limitations, there was a need to control the aspect ratio of micro channels. The control of aspect ratio was advantageous for some applications and disadvantageous for some other applications.

Another process used to seal the samples is PDMS sealing. There are many advantages of using the PDMS bonding when compared to anodic bonding, including

cost-efficiency. Bjorn et al. [46], discussed in detail the physical and chemical properties such as "elasticity, optical transparency, flexible surface chemistry, low permeability to water and low electric conductivity". Every parameter was found to be very suitable as a material for bonding on the top of micro fluidic devices. Many researchers have successfully bonded this PDMS with different materials in wide range of applications.

McDonald et al. [47], mentioned that because PDMS (polydimethylsiloxane) is transparent, it can be used for prototyping micro fluidic devices. McDonald et al., also mentioned that PDMS has numerous applications and that one single device cannot have all the advantages of PDMS (polydimethylsiloxane). Winnie et al. [48], studied two different types of curing process. First, they cured the PDMS for 90°Cfor 3 hours and in another process they cured the PDMS for 20 hours at room temperature. Both showed good bonding strength. The validation of this process was checked by injecting the colored dyes into the micro channel to check for any leakages. According to Eddings et al. [49], instead of traditional oxygen plasma bonding technique, another method such as corona discharge, partial curing, cross linker variation, or uncured variation can result in better bonding strength. The implemented fabrication process was straightforward and was successfully completed by many researchers for various different applications [42] [50].

4.2 Materials and Methods

4.2.1 Pre-Preparation for Anodic Bonding

Pure silicon is subjected with deposition of oxide layer on the top surface to ensure better bonding capabilities while performing the anodic bonding. As discussed above, the oxide layer will ensure the bond between the two surfaces, glass and silicon, establishing irreversible connections. In this process, a 4 inch diameter silicon wafer with 20.5 mm thickness is used. The deposition of oxide process was done using Protemp Horizontal Furnace at the Purdue University clean room. Before starting

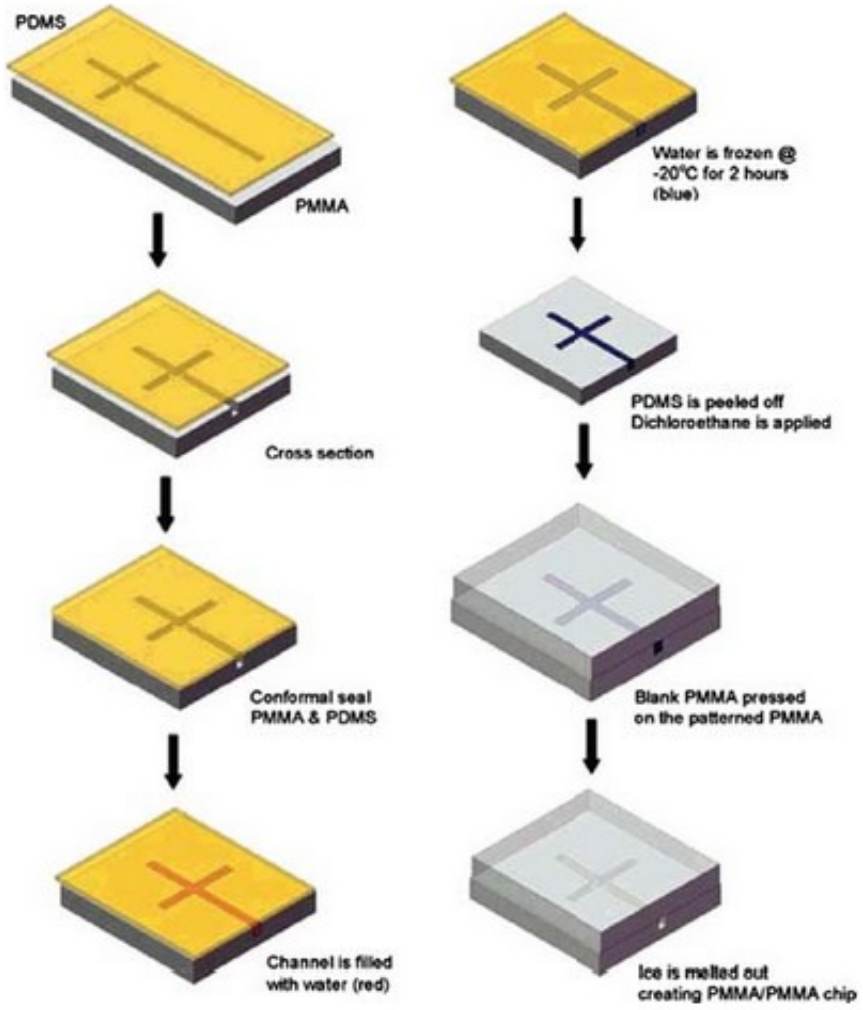

Figure 4.4. Process of PDMS bonding [51]

the actual process, the oxide layer of 220 NM is deposited and the wafers are cleaned using the piranha cleaning process; this process is clearly explained in the following part of this chapter.

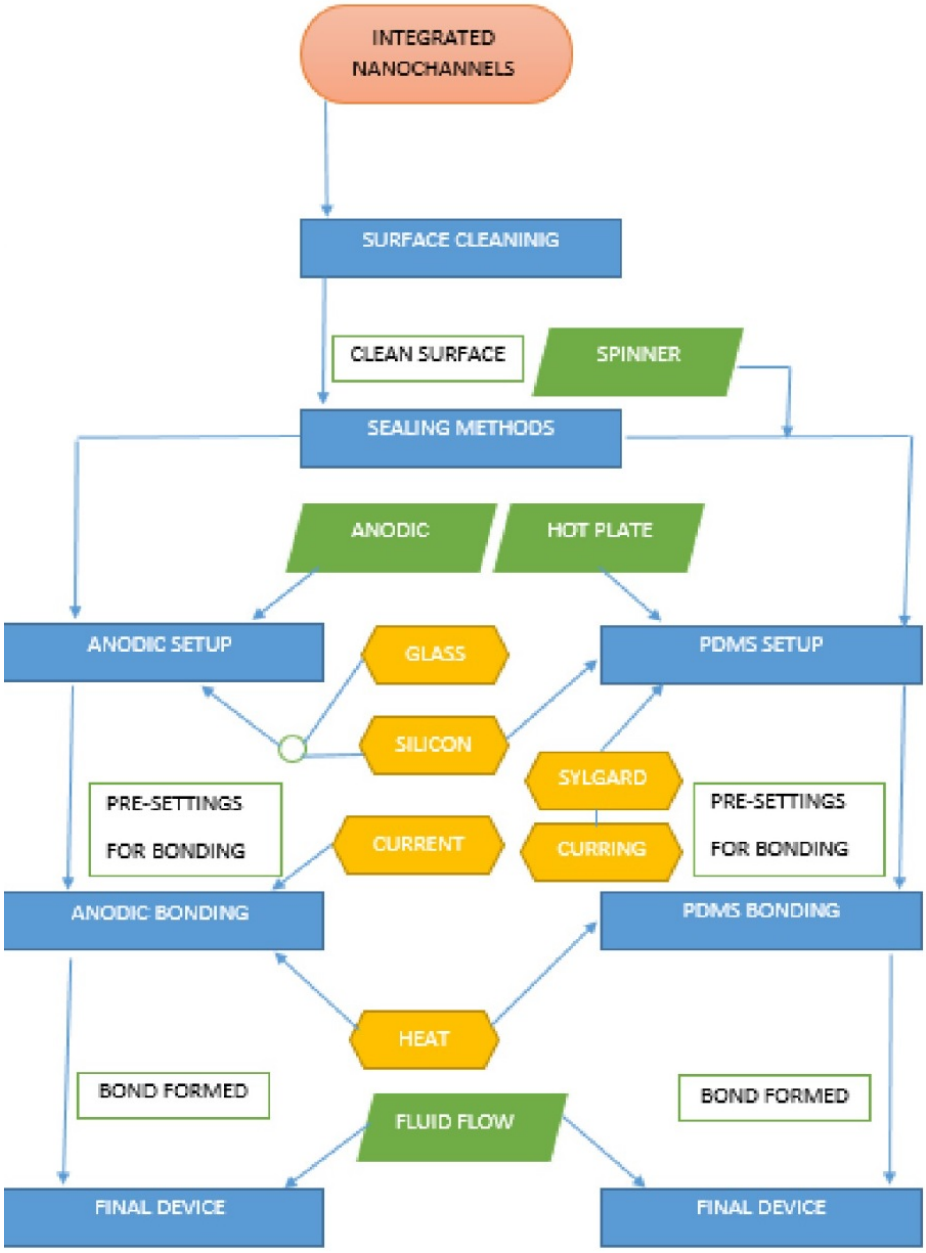

Figure 4.5. Process flow for sealing technique

4.2.2 PDMS Bonding

PDMS bonding is a very effective and direct bonding technique for closing the microfluidic devices. PDMS is a flexible elasto-polymer suitable for microfluidic device. We will use Sylgard 184, a form of PDMS elastomer.

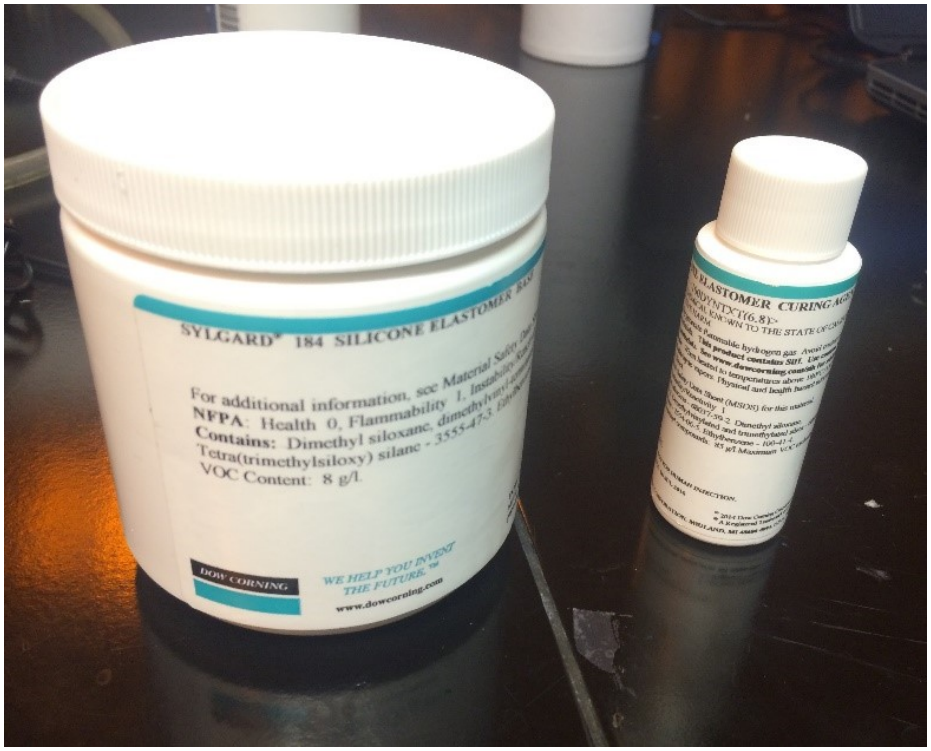

Figure 4.6. Sylgard 184

Sylgard 184 comes with two liquids: a dimethyl siloxane is formed when we mix the vinyl group, and a hydrosiloxane group is present in the bottles. A bond is formed between them, as shown in Figure 4.8, which will be easily bonded with other materials in the desired shapes. The PDMS can be cut into pieces by any sharp metallic structure, such as a blade. To open the inlet and outlets, we can drill a small hole with a needle and insert tubes. This setup will be very supportive to seal the surface of a microfluidic device at an affordable cost.

To prepare the mixture, we mix the curing agent and the polymer base at the ratio of 1:10. A coarse scale is used to measure the weight of the two materials. The solution is mixed for 2-5 minutes with a fork to make sure that it is finely mixed. The solution is poured on the top of the flat disk slowly without any air gaps in between them. The fall disk is then subjected to spin at 1000 rpm for 10 seconds to get a thin

layer of PDMS. Once all the bubbles have been removed, this disk is kept on the top of a hot plate for and cured for 2 hours.

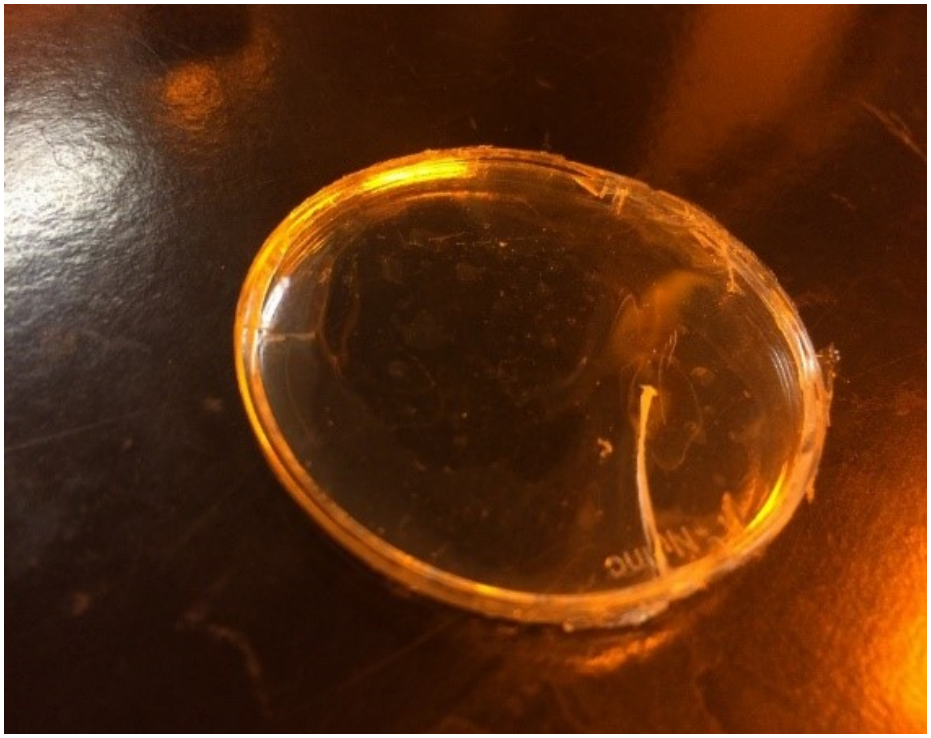

Figure 4.7. Polymer after curing

Using a knife or tweezer, we remove the PDMS from the top of the circular plate and slide it up on the other side. A layer of silicon is coated on the device upon which this PDMS will be bonded. We placed the PDMS on top of the silicon with the tweezer and kept it on top of the hot plate for 5-10 minutes at 70 degrees Celsius.

Fluid flow test was done at INDI (Integrated Nanosystems Development Institute) facility at IUPUI (Indiana University Purdue University Indianapolis). SP101L syringe pump was used to pump the fluid through 0.05in internal diameter pipe which is connected to inlet reservoir of micro channel as shown in Figure 4.9, Figure 4.10. When the fluid is poured inside the pipe with 50 microns/second velocity, it passes through the micro channels and nano channels and get is collected at outlet reservoir of micro channel as shown in Figure 4.10.

Figure 4.8. PDMS (Polydimethylsiloxane) sealed on the micro channels

Holes are specially drilled with micron diameter syringe on the top of PDMS (Polydimethylsiloxane) which is sealed on the top of the silicon.

Figure 4.9. Test setup

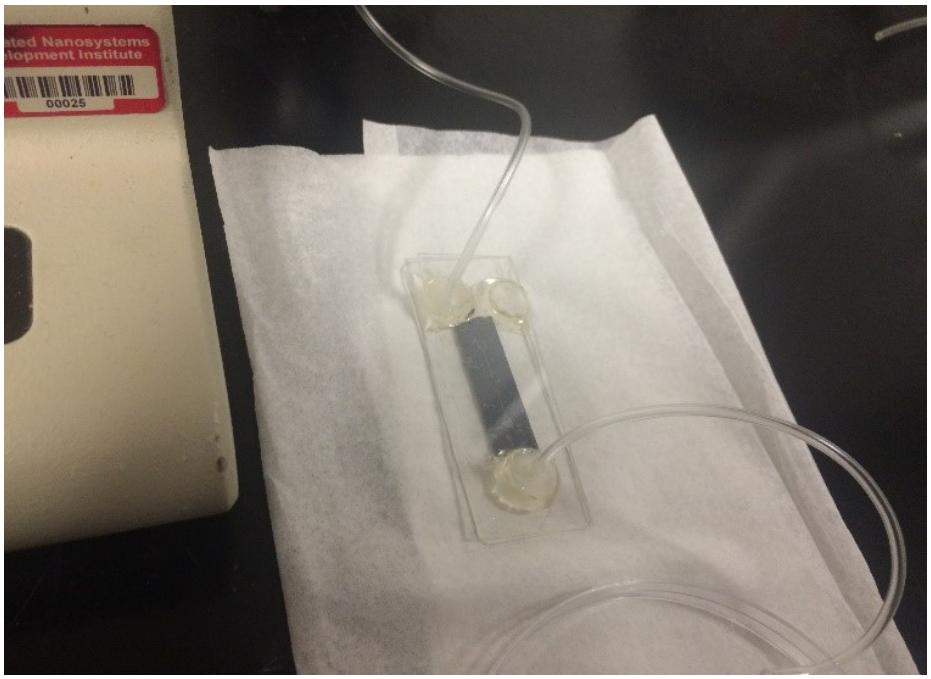

Figure 4.10. Pipes connected to inlet and outlet of device

Figure 4.11. Device after fluid test

5. RESULTS AND DISCUSSION

5.1 Fabrication of Micro Channels

A photolithography process is used to create micro channels on top of the silicon wafer. It is crucial to ensure that the method we have utilized in this process is correct. Photomask was designed in AutoCAD and fabricated at Photosciences Inc. Figure 5.1 displays the chrome coated photomask which is used to transfer the image of the micro channels onto the silicon substrate. This present chapter will discuss in detail what has been achieved in this study. In total, four microfluidic devices have been developed with the same geometry but with different top material. These results will improve understanding of the manufacturing process of micro fluidic devices within which nanofluidics will be integrated.

5.1.1 Inspection of Micro Channels After Photoresist Application

A silicon wafer coated with photoresist is exposed to ultraviolet radiation. On exposure, the chemical process makes the exposed part of the photoresist easy to remove when it is treated with developer. After spinning the wafer for 5 seconds at 500 rotations per minute and 40 seconds at 3500 rpm, it became around 2 microns thick. The exposure of ultraviolet radiation has been performed in contact mode. During this contact mode, both the mask and the glass are in contact when the rays pass through the transparent surface onto the silicon wafer. The light is exposed with an intensity of 14 MW/cm2 at 405 nm for 18 seconds. The resultant thickness of photoresist detected is shown in the following chart. We can calculate the thickness of photoresist with the help of imaging equipment such as atomic force microscopy or any other microscopy techniques.

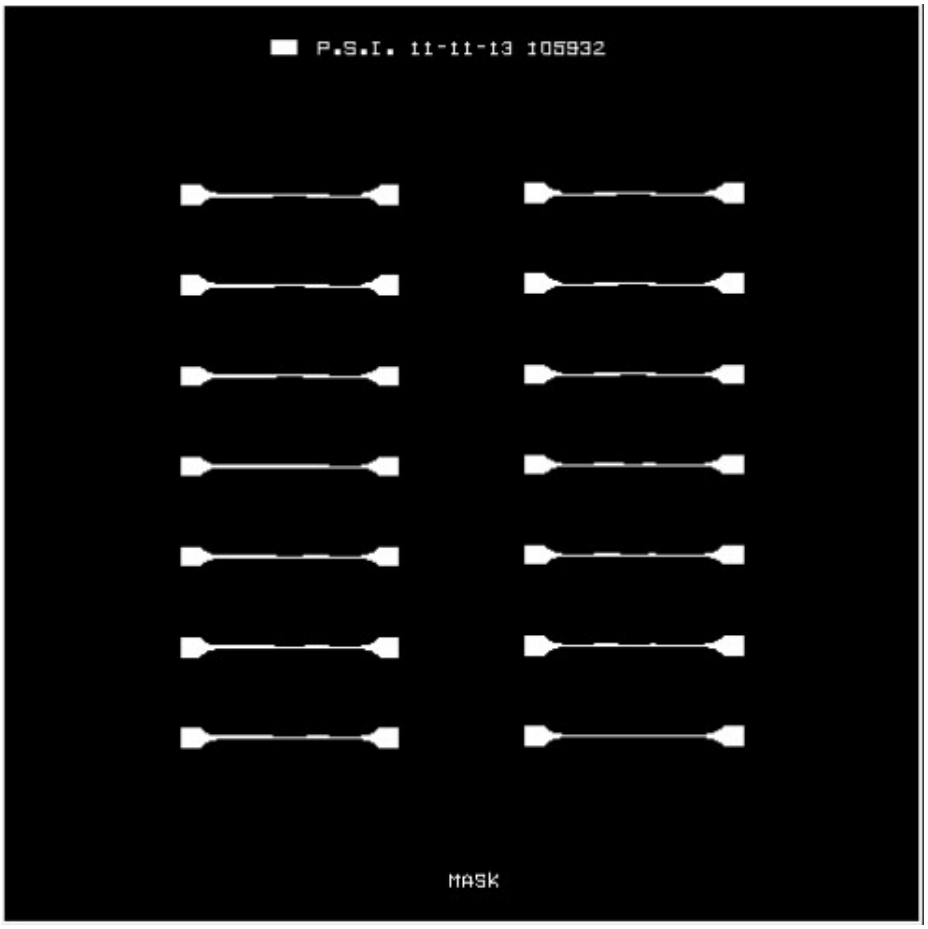

Figure 5.1. Photomask

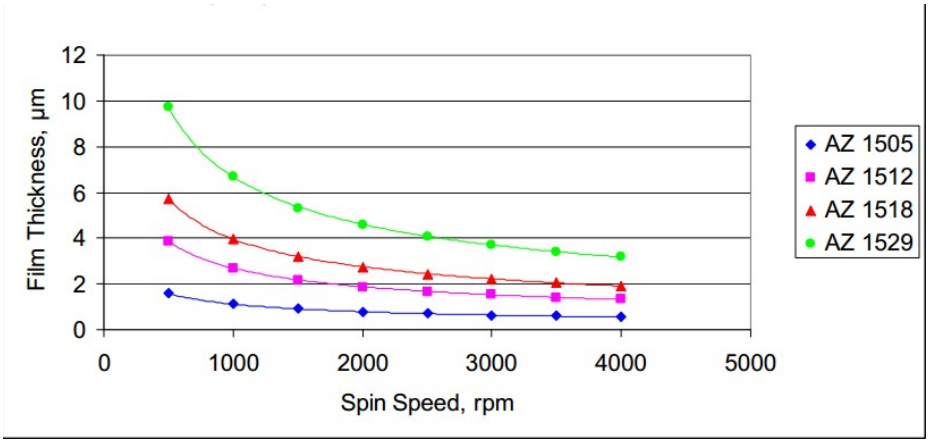

Figure 5.2. Speed vs Thickness spin curve for AZ 1500 photoresist [52]

Table 5.1. Formula used for deposting the photoresist application

STEPS	Time (Seconds)	Speed (Rotations per minute)
STEP 1	5	500
STEP 2	40	3500

Photo mask, which we used for transfer of images, has a dark chrome side and a transparent side. When the light is exposed, it travels through the transparent medium and strikes the photoresist. Being a photosensitive material, the exposed surface becomes harder and can be erased by using a photoresist developer. The MF-26A is filled in a small tumbler, and the silicon wafer is inserted for 30 seconds. It is cleanly rinsed with water after development and inspected in the microscope.

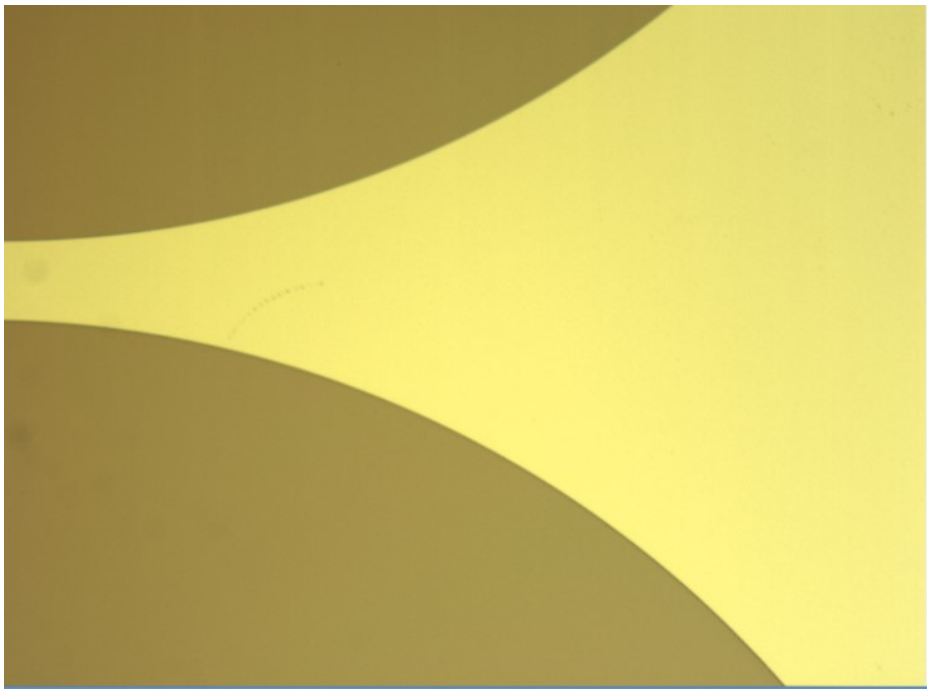

Figure 5.3. Micro-structure of reservoir on photoresist layer

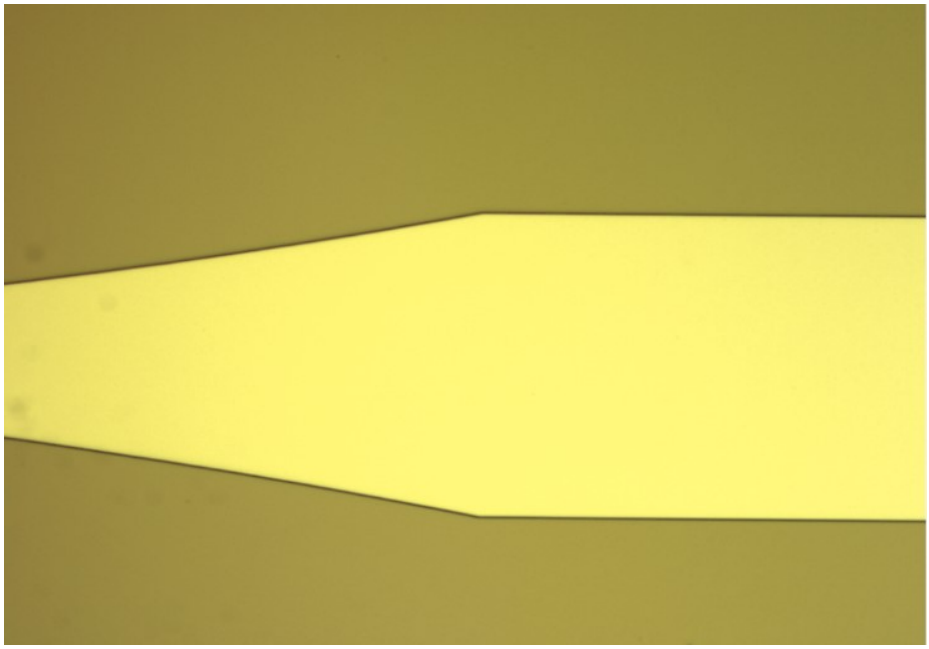

Figure 5.4. Micro channel formed photoresist layer

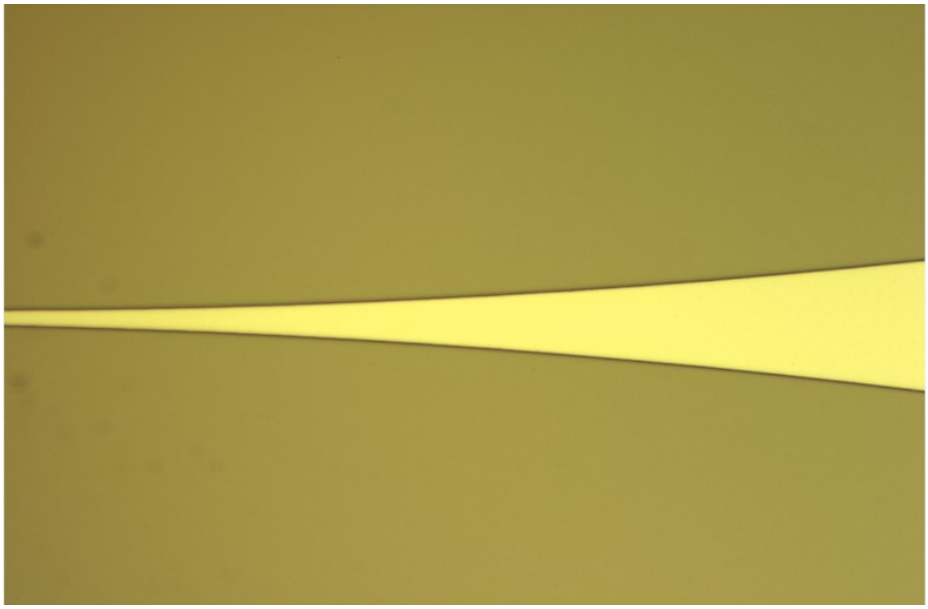

Figure 5.5. Narrowing of micro channel to increase the directionality

5.1.2 Micro Channels After Etching Process

Reaction on etching is used to remove the silicon material to form the micro-channels. Reactive ion etching is an anisotropic process that has better selectivity

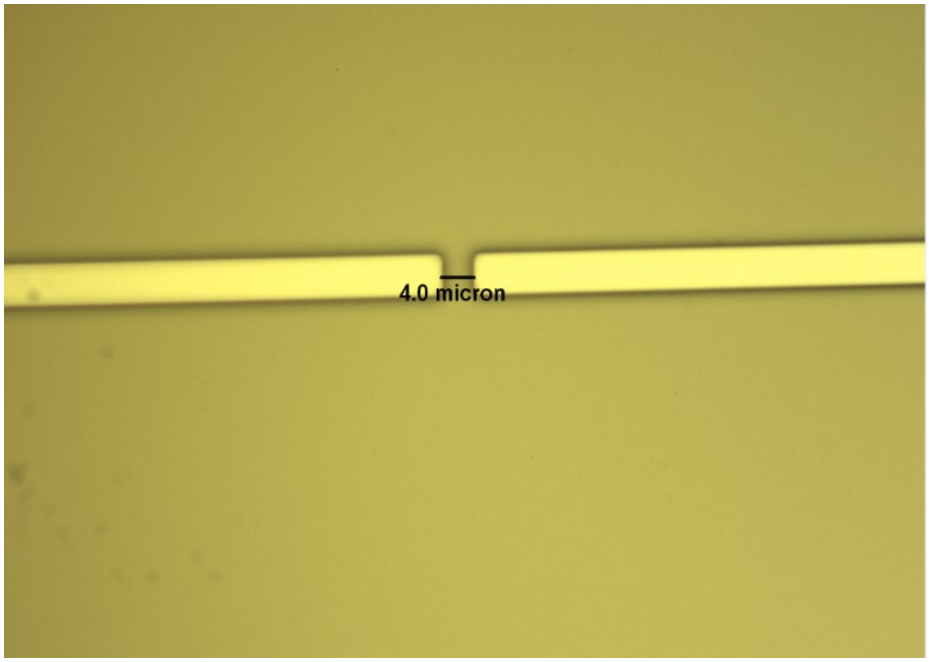

Figure 5.6. Space is left in between the two micro channels to integrate the nano channels

and a much precision when compared to wet etching process. Temperature is a very important factor for the rate of reaction. Mostly, wafer temperature will depend on the chuck temperature, ion's energy, and density. For etching the silicon, we used STS ASE DRIE at the nano fabrication lab at the BIRCK nanotechnology center at Purdue University. It is a 6" ICP process mainly used for removing the silicon.

The etch rate is approximately around 8um/min for 500 UM feature size 20% exposed area, high selectivity to PR 75-100. Micro channels are inspected with optical microscope, and scanning electron microscope images show the sharp vertical micro channels that were achieved with precision after the etching process. The optical microscope will be pre-set to the zoom level at which the best images can be captured.

The thicker boundary lines represent the thickness of micro channel. A uniform thickness has been achieved from 10-12 micro meters, shown in the images captured by scanning electron microscopy.

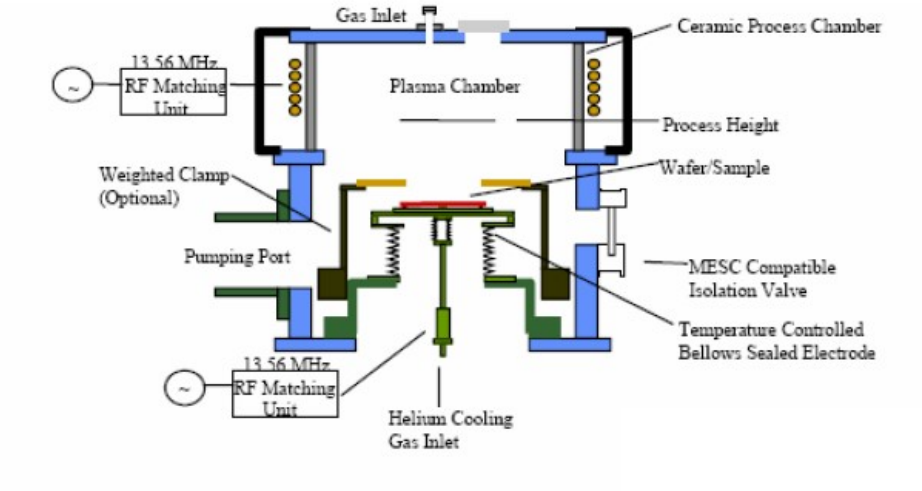

Figure 5.7. Detail of level parts of RIE equipment [33]

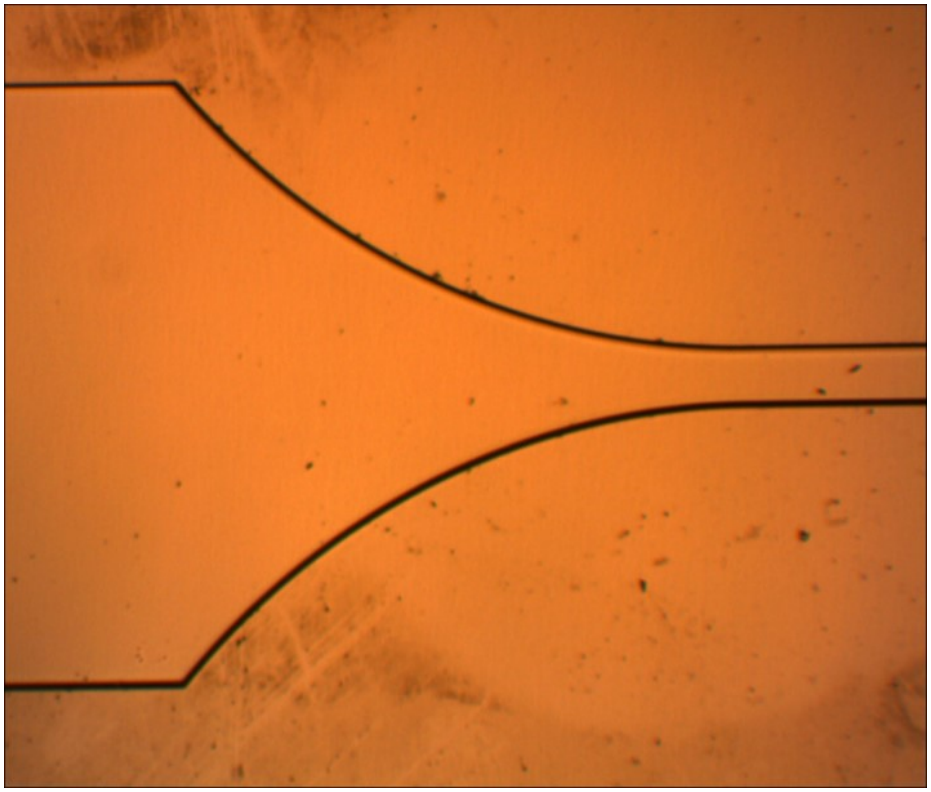

Figure 5.8. Reservoir captured with optical microscope

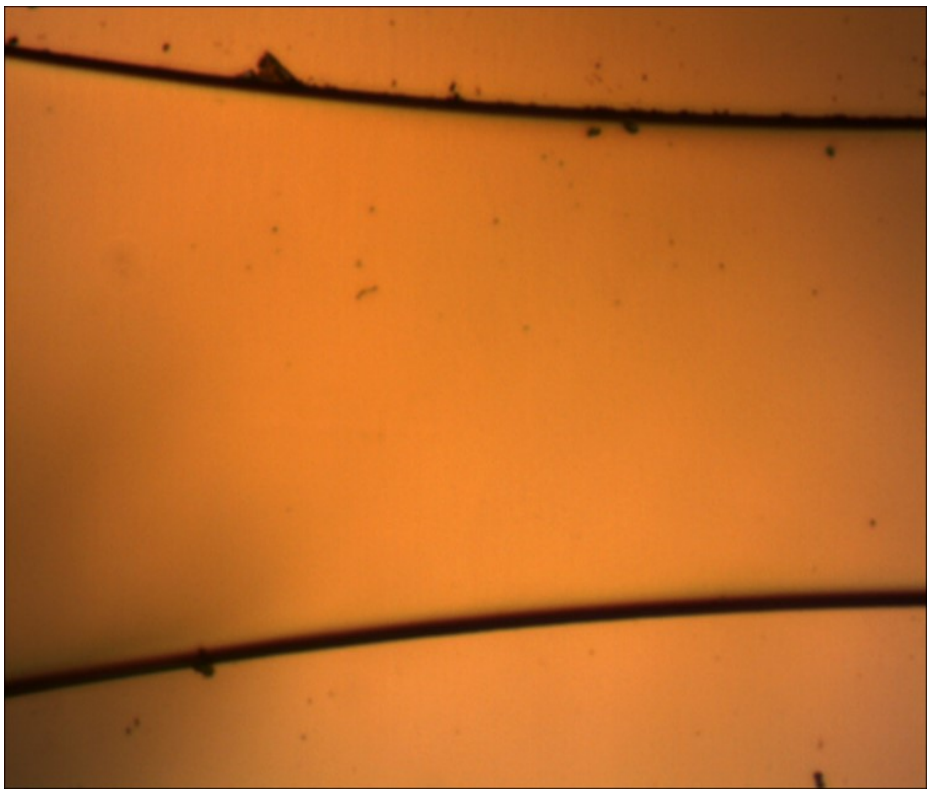

Figure 5.9. Middle region of micro channels captured with optical microscope

The scanning electron microscope allows only a limited size of the sample inside the vacuum chamber where the images are captured. To capture the cross sectional view of the micro channel, we have dedicated a sample by breaking it into two parts. The sample was cleaned with acetone to remove broken silicon pieces and other dust particles.

Each wafer can be sub-divided into 14 microfluidic devices. The integration of nanofluidics will be done in the space between the two micro channels, as shown in the Figure 5.12.

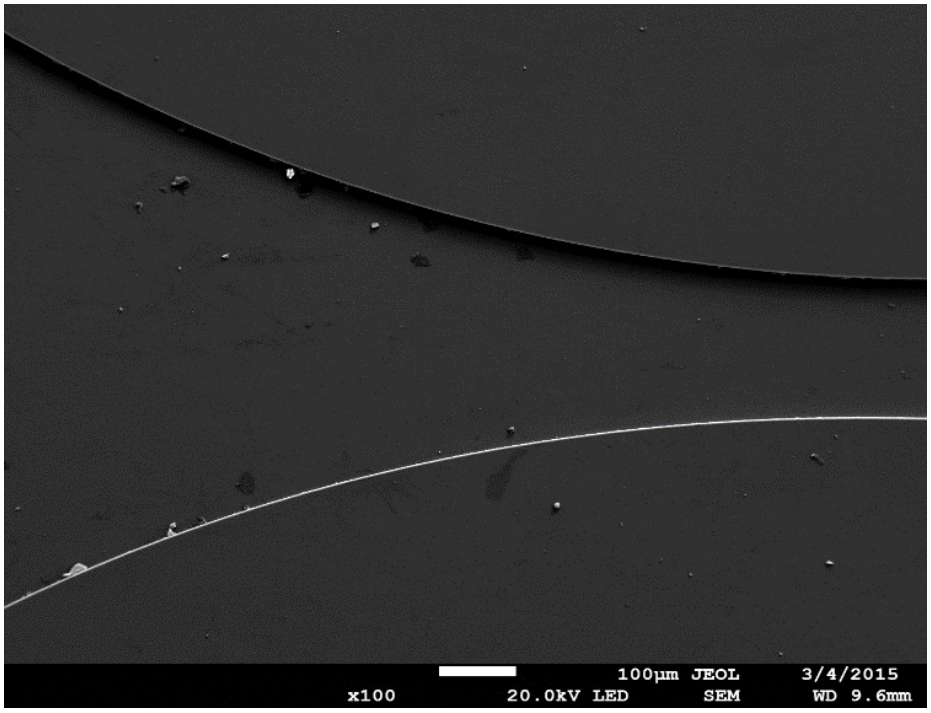

Figure 5.10. SEM image of micro reservoir

Table 5.2. Comparison of fabricated micro channels and the space between them

Achieved spacing between micro channel	Depth of the micro channel	Number of device per silicon wafer
4	10	6
5	10	4
6	10	2
7	10	2

5.2 Fabrication of Nano Channels

5.2.1 Deposition of Photoresist

A layer of photoresist S-1813 is used as a layer on the top of the silicon microfluidic device to prepare the surface for nano scratching. After the surface cleaning step, the

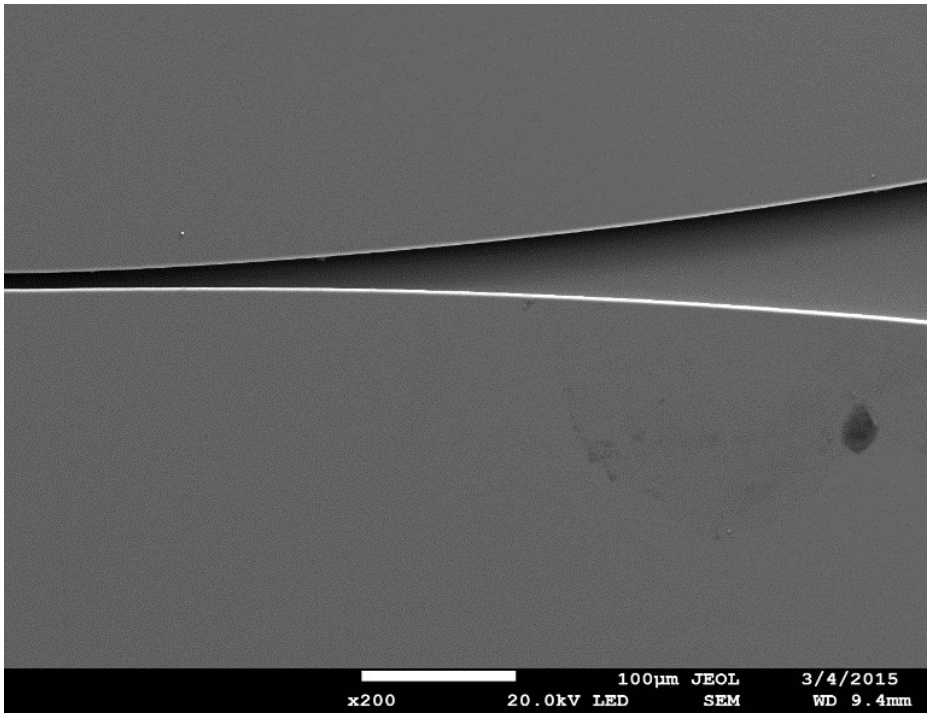

Figure 5.11. SEM image of narrow micro channels

Photoresist S-1813 is subjected to spinning on the top of the silicon device with 500 rpm for 10 seconds, followed by 8000 rpm for 45 seconds. This unique way of spinning formula was formed after careful observation of the thickness behavior on the top of the silicon surface. A layer of approximately 2 microns was formed on the top of the wafer. This layer will be used for scratching with help of atomic force microscopy, which will offer more clarity.

The spinning formula 5 seconds for 500 rpm, ramp 3 seconds, and final step involves a spinning speed of 3500 rpm for 45 seconds. A 2000A thick layer was generated on top of the silicon substrate.

A test was performed to check the chemical compositions of material which is captured in SEM. SEM uses X rays to better identify the deposition of materials. Figure 5.7 represents three selected areas after observing the chemical properties from the resultant material identification graphs. As shown in Figure 5.16 and Figure 5.17,

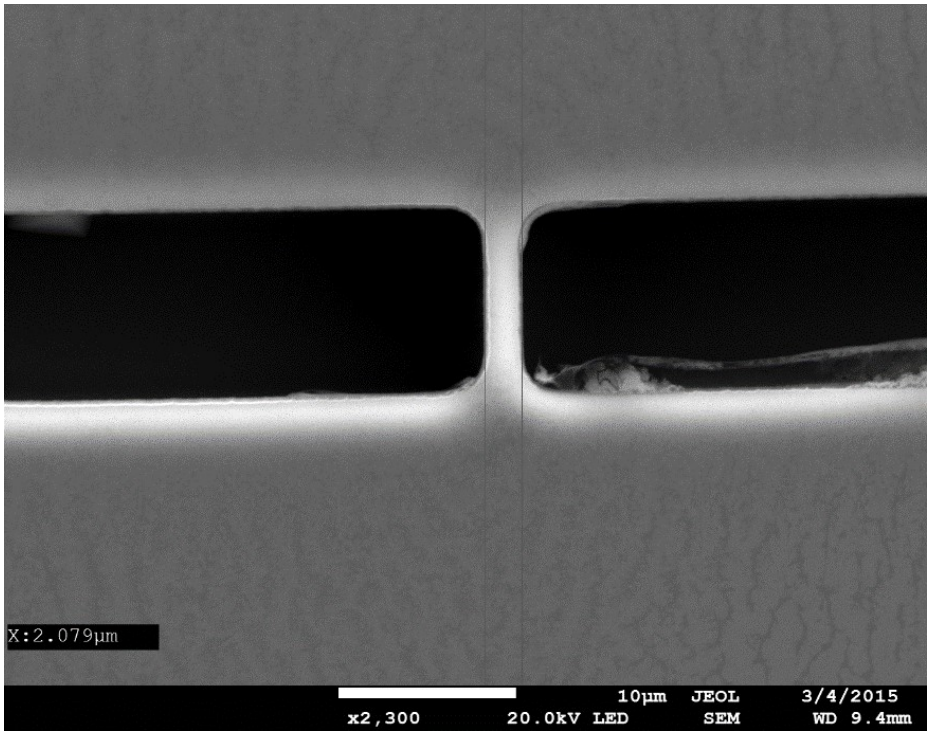

Figure 5.12. SEM image of space between the two micro channels

we can clearly identify the deposition of photoresist on top of the silicon wafer. This test is called [need to add material.

5.2.2 Deposition of Gold Sputtering

A gold layer is deposited on top of a microchannel made of silicon. A magnetron sputtering device is used for the deposition of gold. A magnetron creates optimum conditions for sputtering by controlling the basic pressure at 10-8Torr, arc pressure at 4 Pa, and DC current at 50 watt. The rate of deposition has been performed on the top of a sample. A detailed value on gold sputtering is shown below in Figure 5.20. Argon gas is used to transfer the gold into vaporous state, and it gets deposited on the top of the sample.

To measure the exact thickness of the gold, we used a square silicon sample material on which half of its area is covered by plastic tape. After completing the

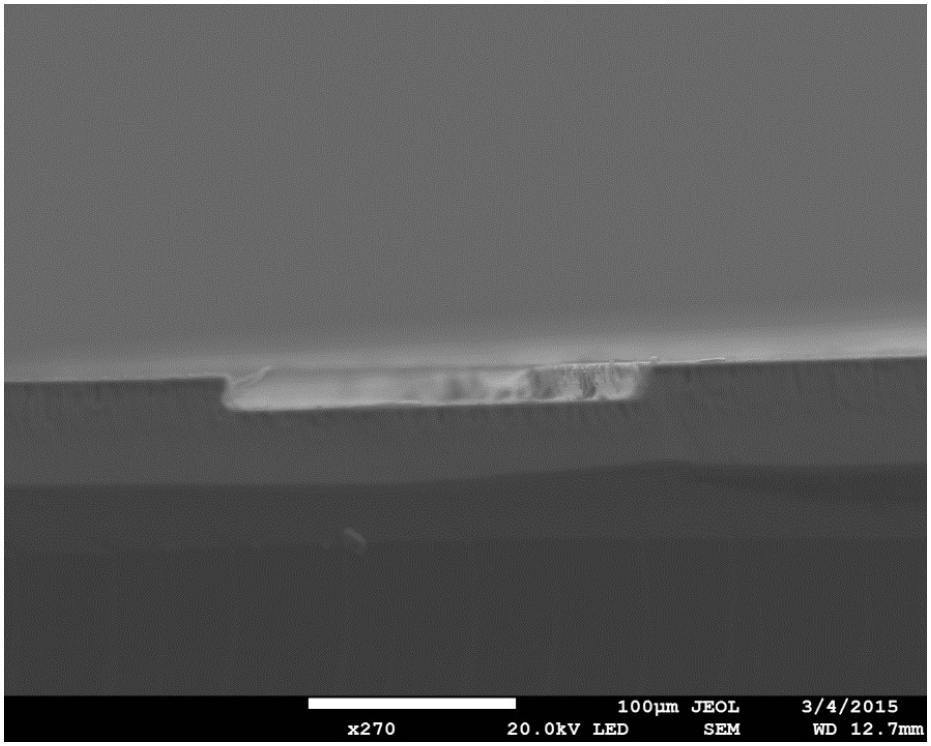

Figure 5.13. Side wall of micro channel captured with SEM

Table 5.3. Deposition of gold layer

Time IN SECONDS	THICKNESS IN NM
30	9
115.7	34.7
667.7	200

experiment, the tape is removed, leaving the other half of the gold. When imaged with AFM, we can easily measure the thickness deposited in the time period. A graph is generated to determine the thickness with precision.

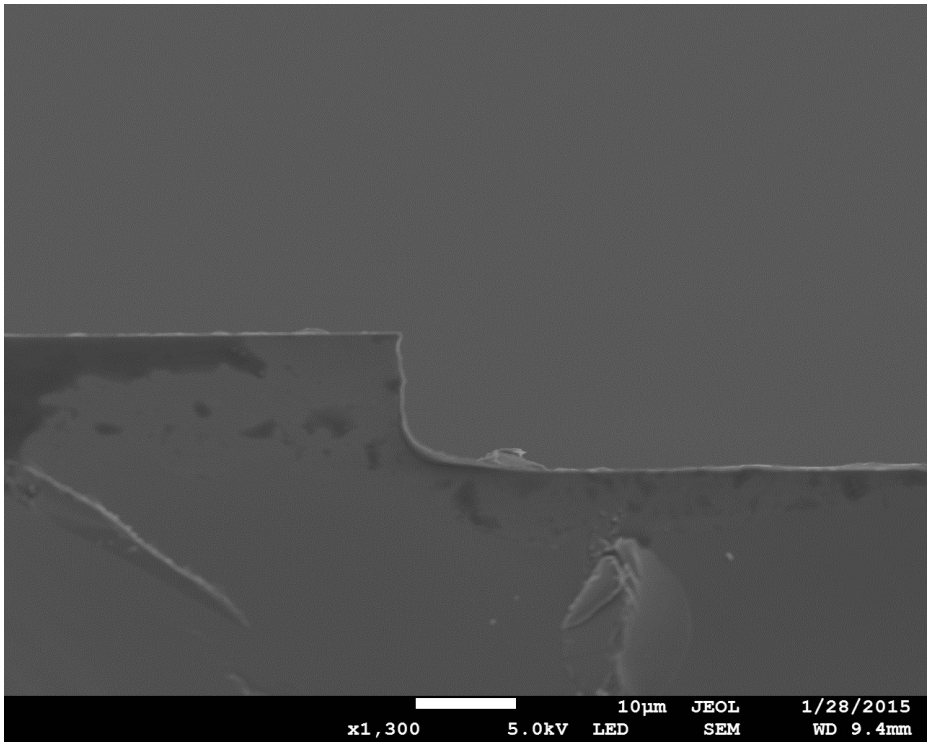

Figure 5.14. Cross sectional view of micro channel

5.2.3 AFM Based Nano Channels

Nano channels have been made by making use of diamond and silicon carbide tip. The below Figure 5.27 briefly explains the results. These nano channels are integrated in the space between the two micro channels. Graphs were also generated with AFM to study the process closely.

Table 5.4. Fabrication of nano channels

S.NO	LENGTH	DEPTH	WIDTH	QTY OF CHANNELS
1	4 UM	100 NM	75 NM	6
2	5 UM	100 NM	75 NM	6

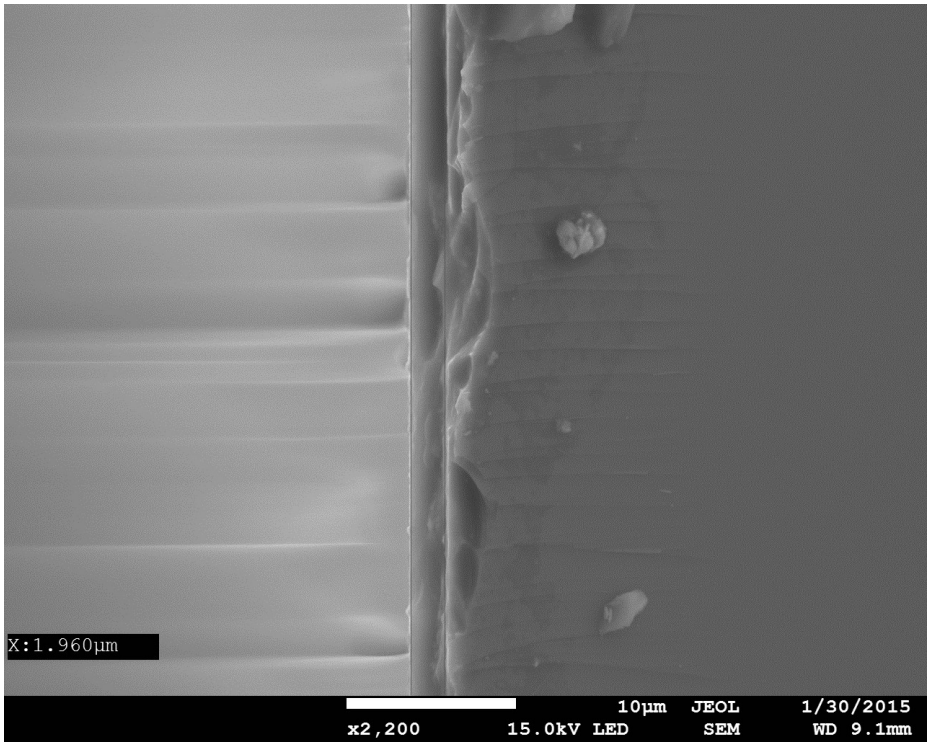

Figure 5.15. 2 um layer of photoresist on the top of the silicon wafer

In the Table 5.4, six nano channels have been fabricated using AFM nano machining process. Diamond tip was used to scratch on the top of the silicon. In sample 1, the length of the nano channel is 4 microns, depth is 100 nano meter, width is 75 nano meter. In the sample 2, the length of the nano channels has been changed to 5 microns, depth and width of the nano channels remain same.

Table 5.5. Fabrication of nano channels

S.NO	LENGTH	DEPTH	WIDTH	QTY OF CHANNELS
1	4 UM	850 NM	90 NM	6
2	5 UM	850 NM	90 NM	6

In the Table 5.5, six nano channels have been fabricated using AFM nano machining process. Carbide tip with silicon cantilever was used to scratch on the top of the

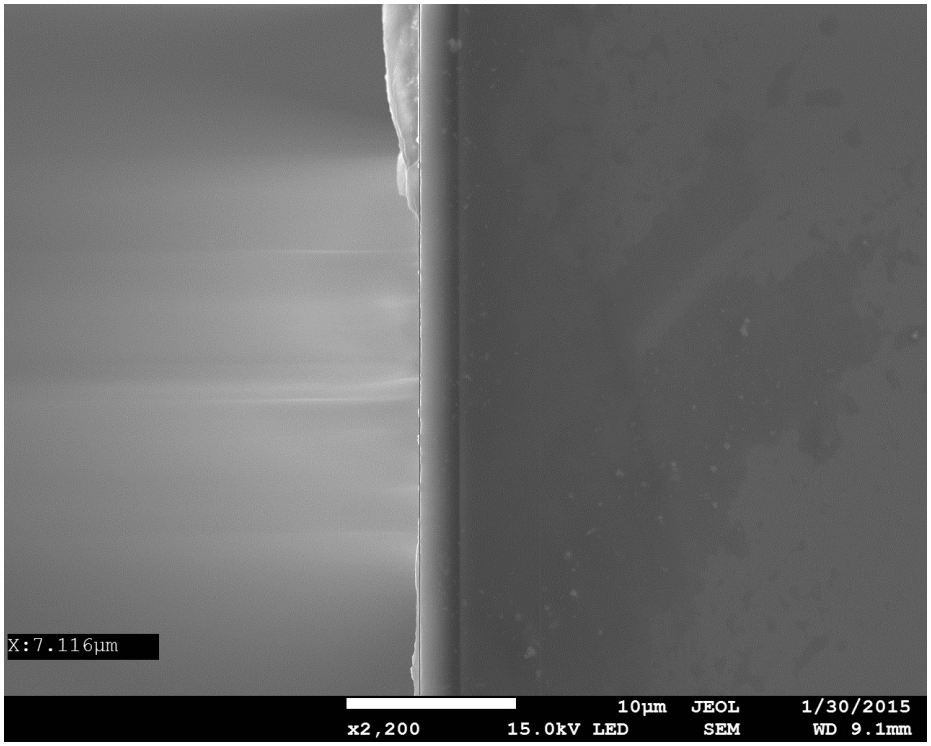

Figure 5.16. Photoresist layer on top of silicon

silicon. In sample 1, the length of the nano channel is 4 microns, depth is 850 nano meter, width is 90 nano meter. In the sample 2, the length of the nano channels has been changed to 5 microns, depth and width of the nano channels remain same.

In the below Figure 5.22, micro channels was detected using AFM image mode. The square red box on the Figure 5.22 indicates the concentration of zoom in particular area. A search has been made to find the 4 micron space between the two micro channels to perform nano scratching using indentation mode of AFM.

To detect the exact center in the Figure 5.23, X1 point from the left micro channel and X2 point from the right micro channels are marked and X center formula has been used which is (X2-X1)/2. By using the X center formula we can get exact center through which we can nano machine the nano channels using indentation mode.

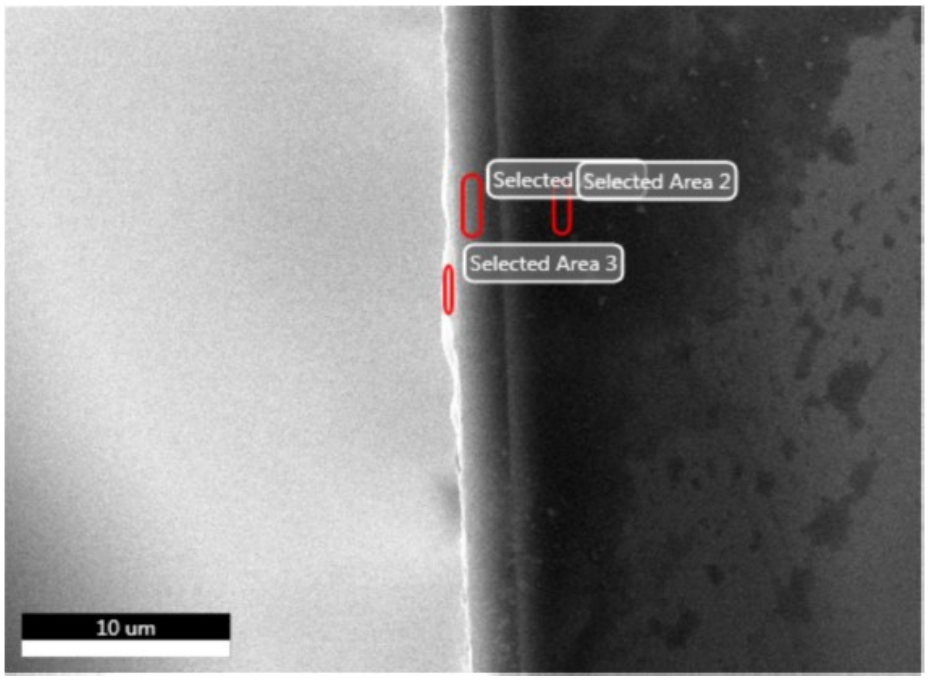

Figure 5.17. Red mark shows the particular parts where this has been slelected

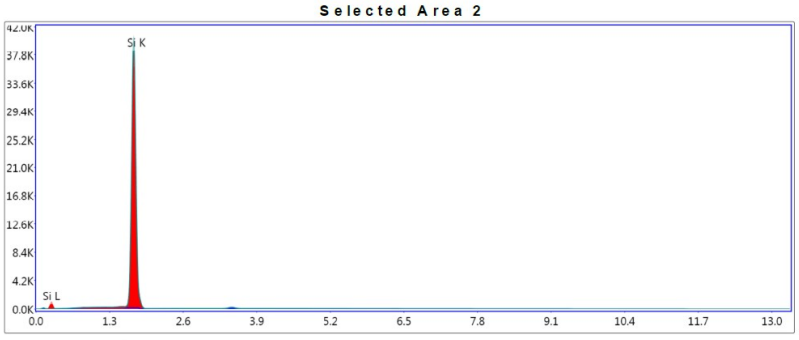

eZAF Smart Quant Results

Elemen t	Weight %	Atomi c %	Net Int.	Error %
SiK	100	100	23334.15	1.09

Figure 5.18. Material identification in area 2

The advantage of machining nano channels are that we have complete control over X-axis-axis and Z-axis at the same time. Figure 5.24 shows a random graph captured during the nano machining process using AFM.

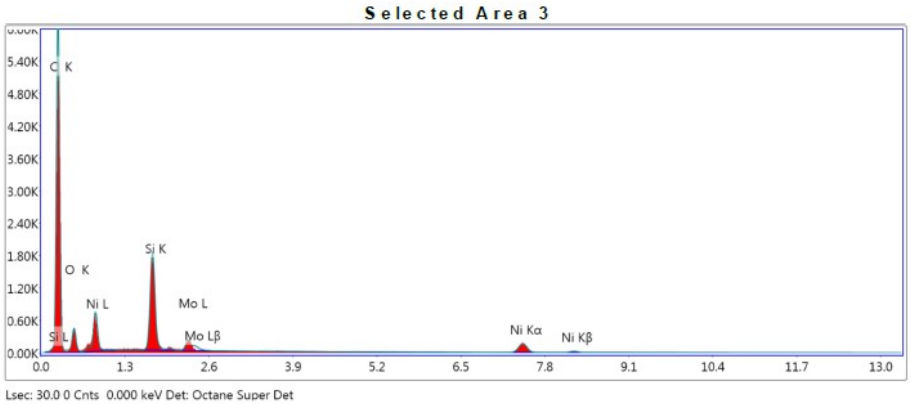

eZAF Smart Quant Results

Element	Weight %	Atomic %	Net Int.	Error %
C K	80.35	88.97	2524.46	6.54
O K	8.98	7.46	158.56	14.43
SiK	5.16	2.44	1103.27	3.13
MoL	1.39	0.19	130.65	8.08
NiK	4.12	0.93	172.21	5.04

Figure 5.19. Identification of photoresist in area 3

As mentioned in the Table 5.4 and Table 5.5, six nano channels have been made with specific length, depth and width depending on our application. Detailed characterization of theses nano channels in the above mentioned tables.

Rapeepan et al. has performed nano machining using AFM on the gold surface to compare the molecular dynamic simulation to experimental results. Diamond tip which is in the shape of pyramid has been used to perform this functionality. Scratching length is 30-90 nm, Scratching depth 1-7nm, tip speed 10 m/s, bulk temperature 293 K, time steps 1 fs (10-15s)

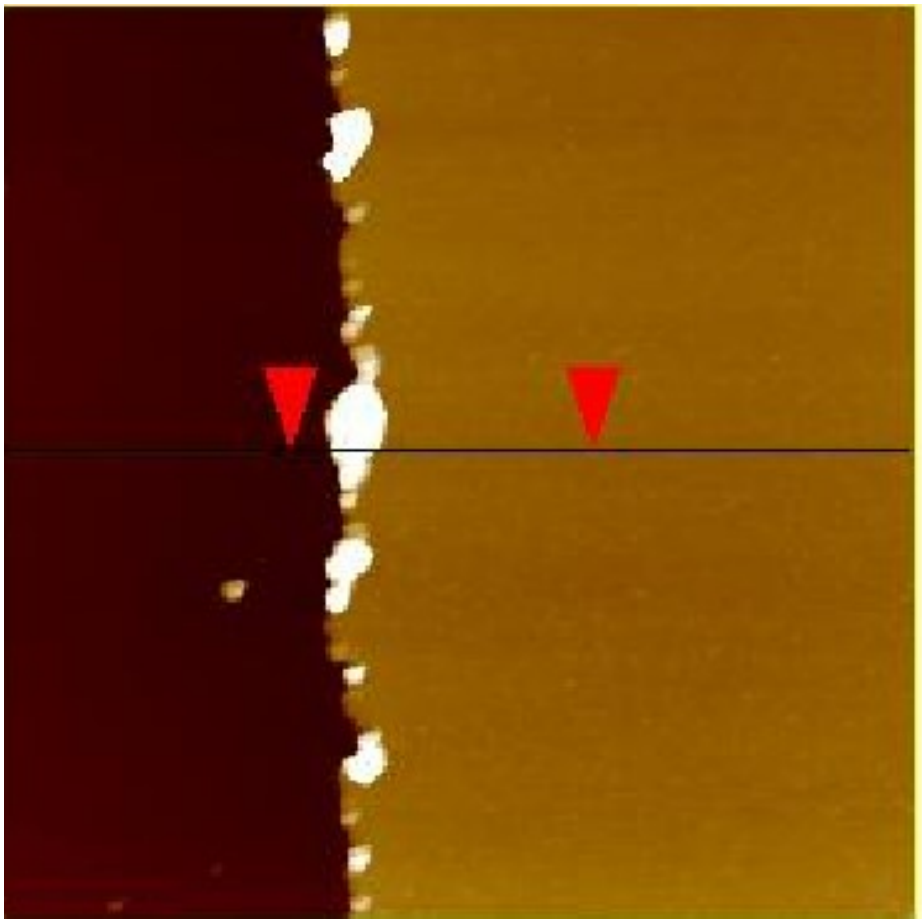

Figure 5.20. AFM image of gold layer deposition

5.3 Cost Evaluation

5.3.1 Evaluation of Lithography Process

A detailed evaluation has been conducted for the time, as it shows a comparison between the traditional lithography process and the new atomic force microscopy. For each operation, the time and cost have been evaluated, as shown in the table and graphs below.

We observed that the graph time associated with the rest of the other process is high. For every time that we wanted to make changes in the dimensions of nano channels, we needed to create a new mask, which consumes more time when compared

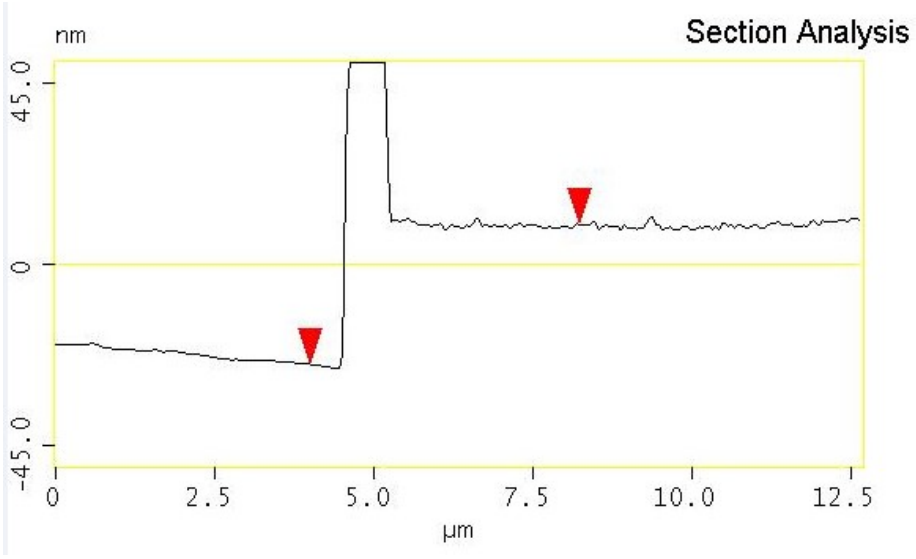

Figure 5.21. Determination of exact thickness gold deposition

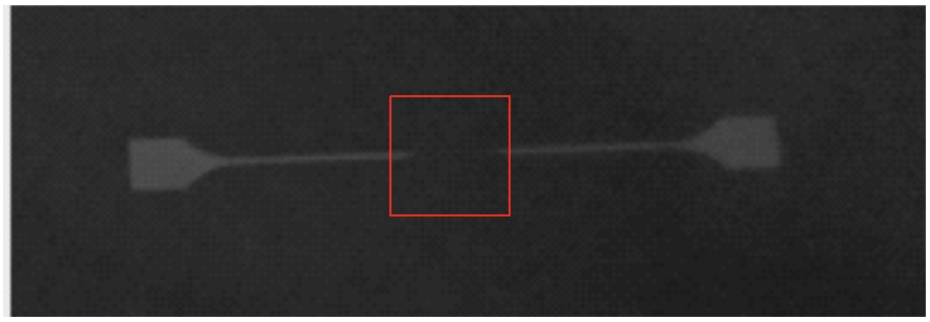

Figure 5.22. Identification of space between two microchannels with AFM

to other process. Etching operations will have control over the depth of the nano channel during the fabrication process. There has to be an advanced lithography process, such as ion beam lithography, which is used in fabrication of nano channels.

The fabrication process is conducted in clean room, which is usually a more expensive process when compared to the regular lab, as it maintains a cleaner environment by constantly filtering the dust particles.

Also, as we can observe in the Figure 5.31, the fabrication of the mask is higher, and a new mask will be created every time we vary the dimensions in 2 dimensions.

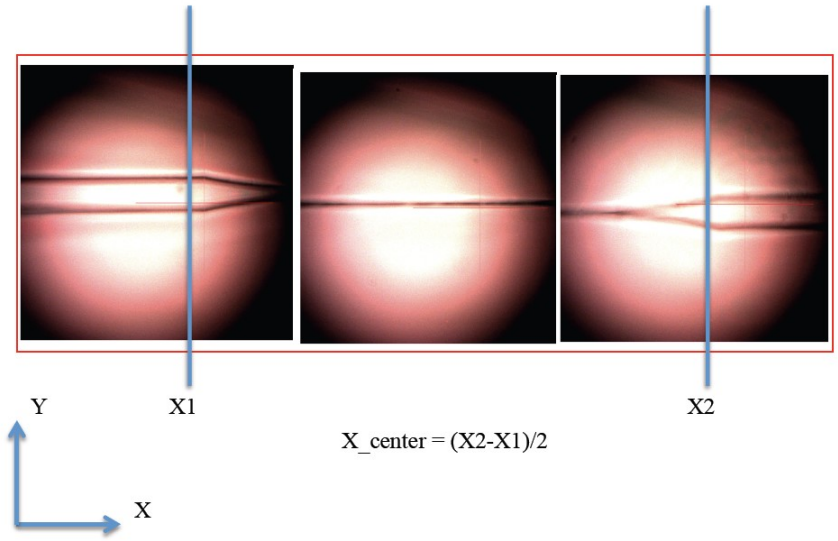

Figure 5.23. Determining the center location for fabricating nano channels

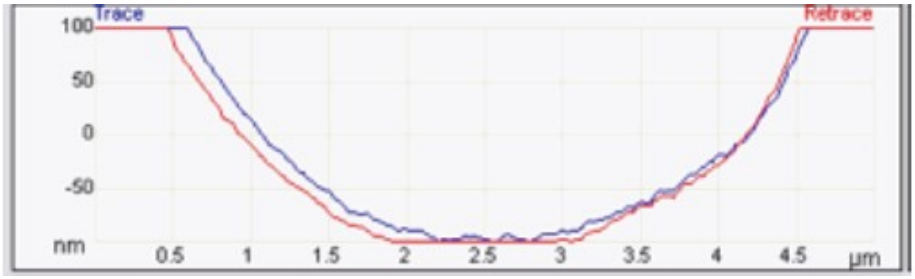

Figure 5.24. Depth vs width

5.3.2 Evaluation of AFM Machining Process

The time and cost involved in fabricating the nano channels using atomic force microscopy were also evaluated.

5.3.3 Comparison Between AFM Machining and Lithography Process

To determine the most affordable method to fabricate the nano channels, we have compared the time and cost involved in complete production, as shown below.

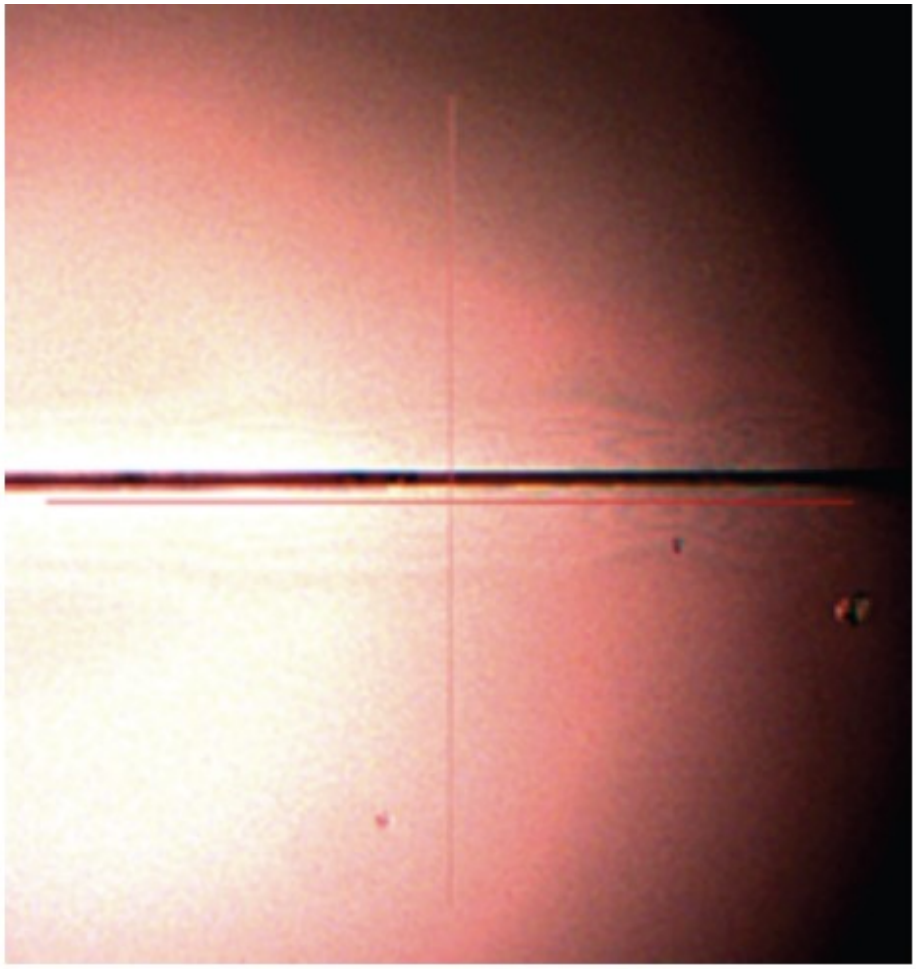

Figure 5.25. Nano channel of 4 um length

The cost of fabrication for the lithography process is very high when compared to the AFM process, as it involves more operations. The equipment used in developing nano channels using lithography process is more expensive when compared to the atom force microscopy.

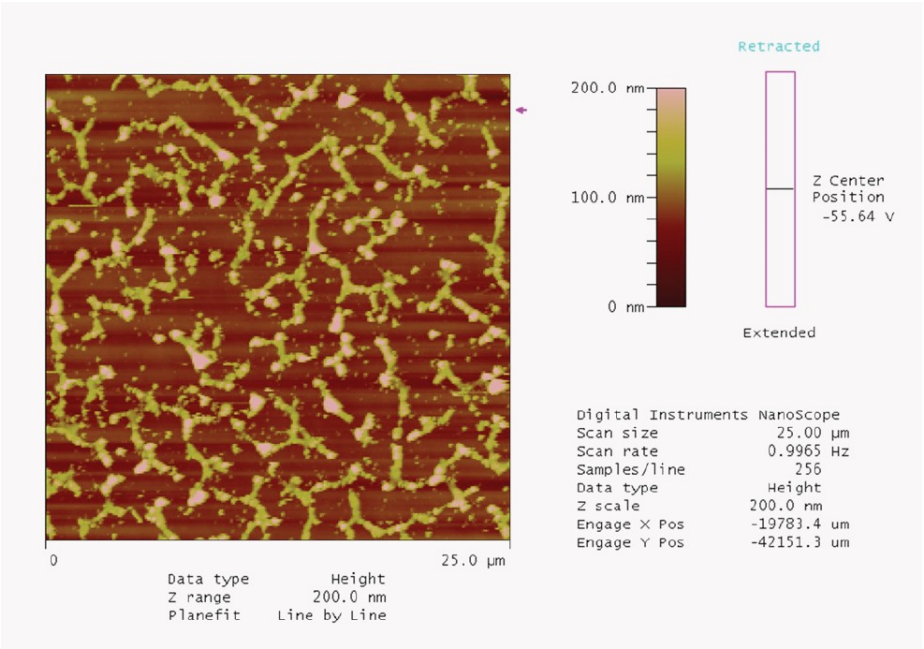

Figure 5.26. AFM image of the surface

Table 5.6. MFG time and MFG cost associated with lithography process

Process	MFG time in minutes	MFG cost in dollars
preparation of photomask	240	400
surface preparation	15	20
photoresist application	45	35
soft bake	3	5
align and exposure	60	180
hard bake	3	5
inspection	60	50
etching	60	218
resist strip	30	0
final inspection	60	120

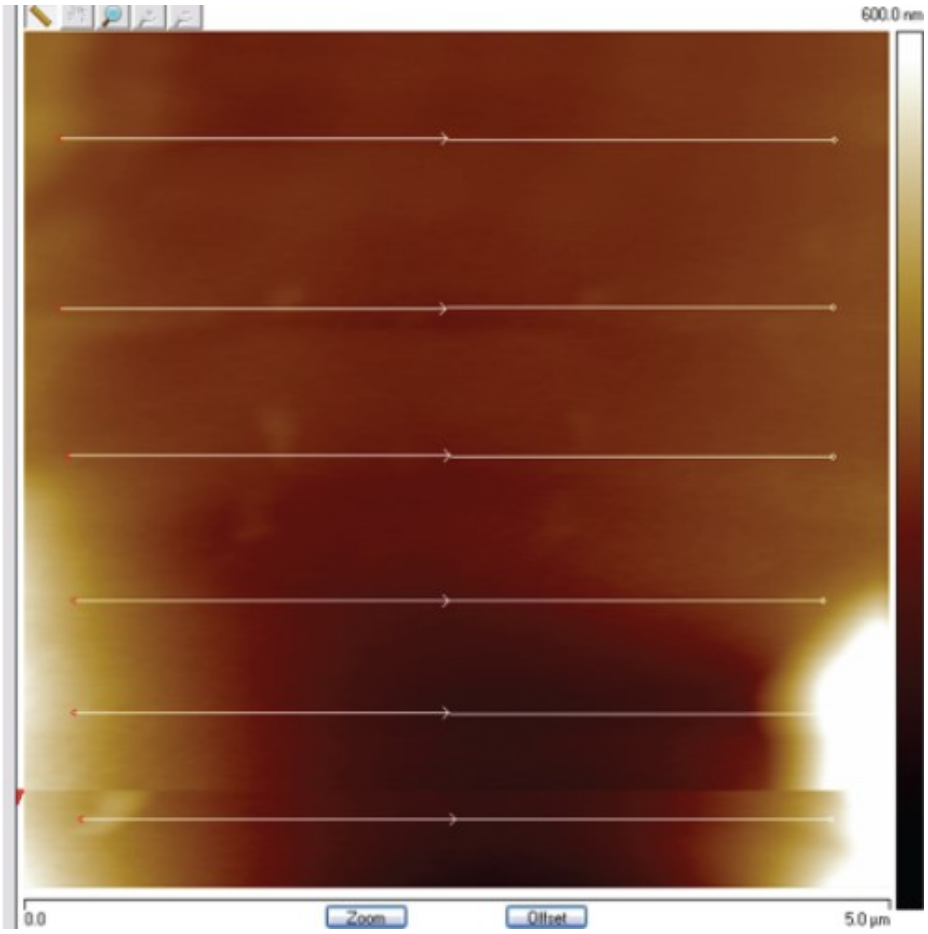

Figure 5.27. AFM image of nano channel

Table 5.7. Shows total time and cost associated with the lithography process

Lithography Process	evaluation	units
Total time	576	minutes
Total cost	$1,023	dollars

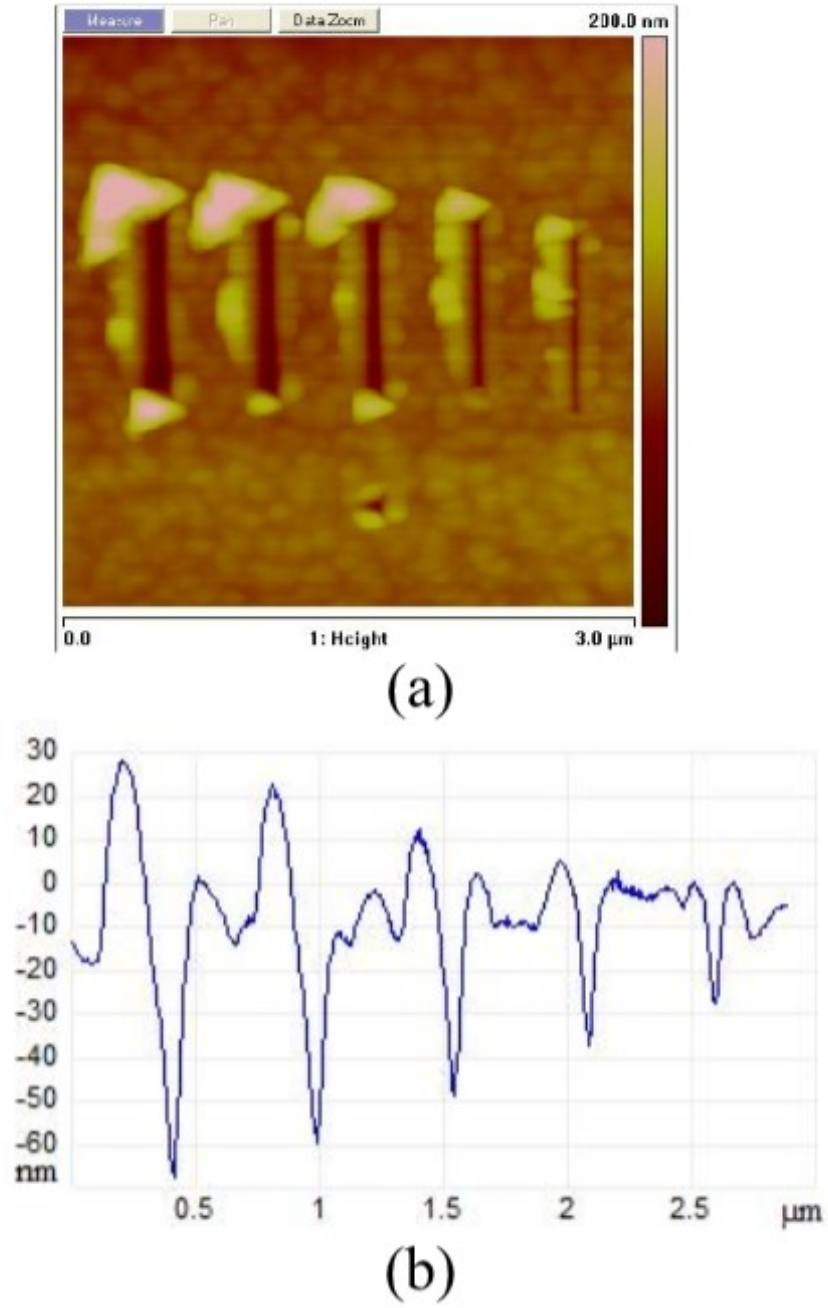

Figure 5.28. AFM experimental results for nano scratching [34]

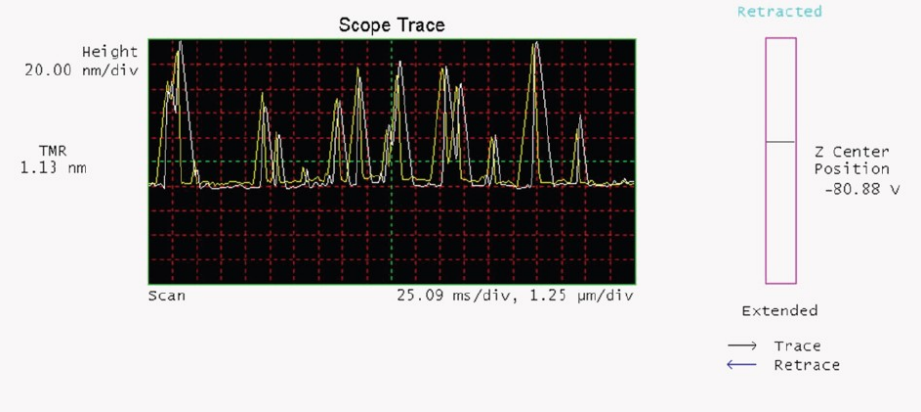

Figure 5.29. Surface scanning of sample with AFM [34]

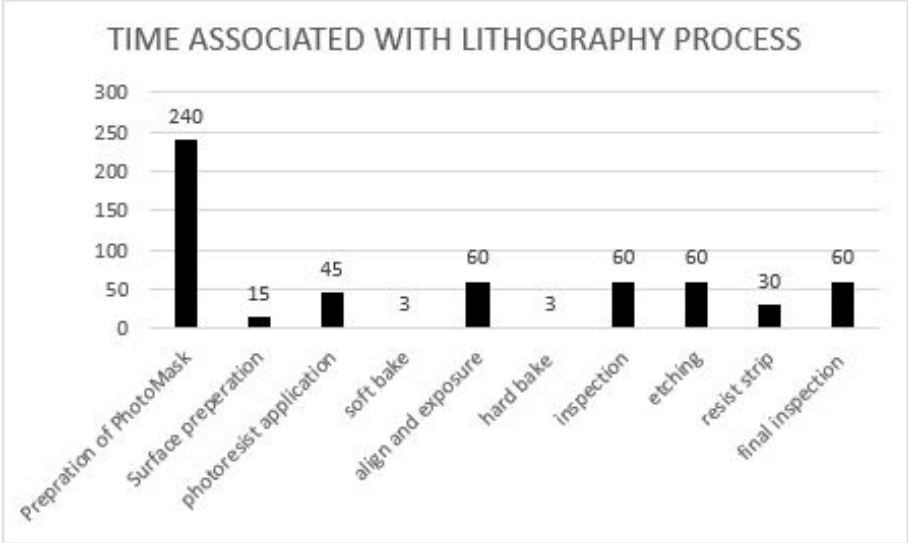

Figure 5.30. Operation time in minutes spent during lithogrphy

Table 5.8. MFG time and MFG cost associated with lithography process

Process	MFG TIME	MFG COST
Surface cleaning	15	20
deposition of material	60	50
tip selection	20	350
Usage of AFM	180	200

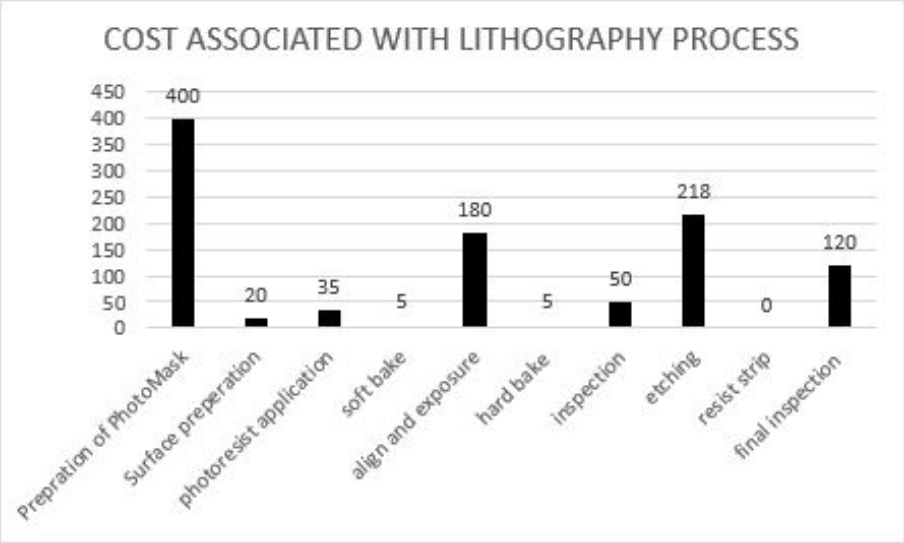

Figure 5.31. Operation cost in dollars spent during lithogrphy

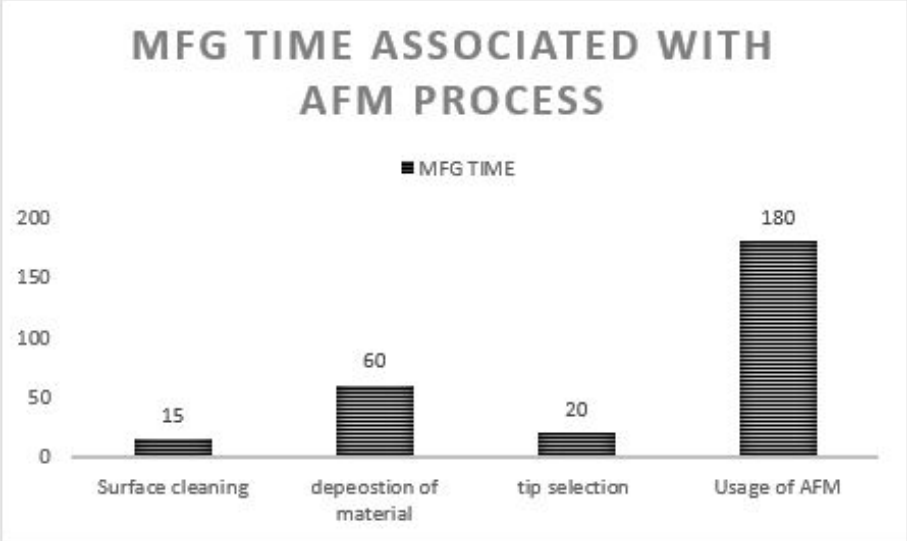

Figure 5.32. MFG time spent during AFM process

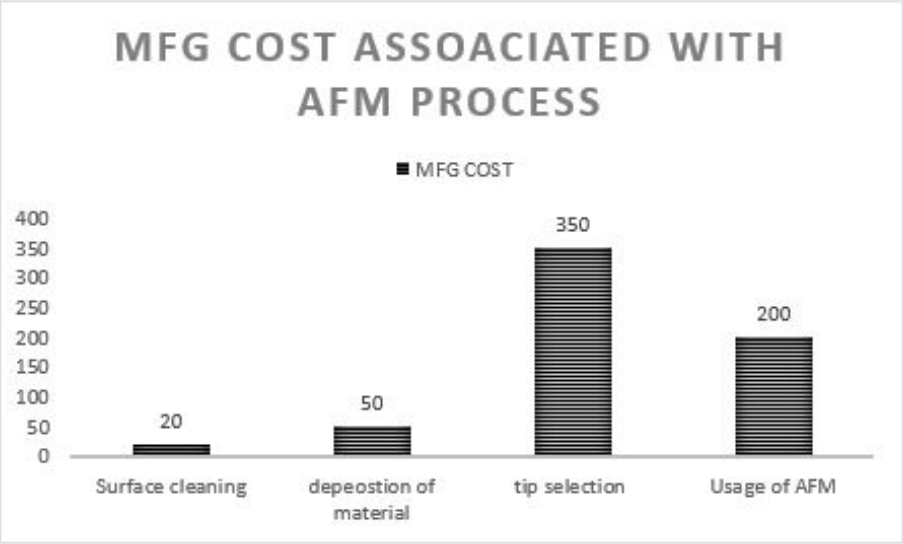

Figure 5.33. Cost associated with AFM machining process

Table 5.9. Differences in time between AFM machining and lithography process

Method	QTY	UNITS
Total AFM time	275	minutes
Total lithography time	576	minutes
Total time savings	301	minutes
Time saving in percentage	47.74305556	%

Table 5.10. Cost difference between AFM machining and lithoraphy process

compression	QTY	UNITS
Total AFM cost	620	dollars
Total lithography cost	1023	dollars
Total time savings	403	dollars
Time saving in percentage	60.60606061	%

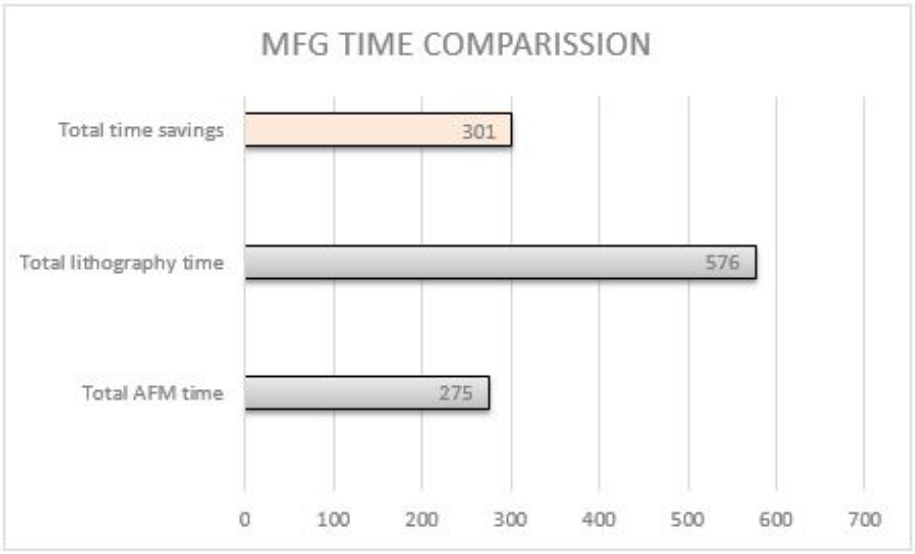

Figure 5.34. MFG time between AF machining and lithography process

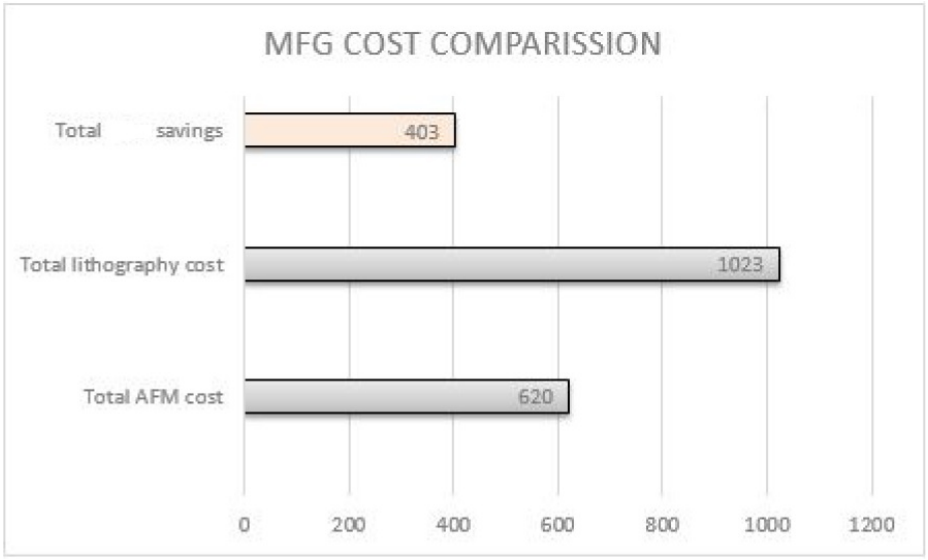

Figure 5.35. Cost comparison between AFM machining and lithography

6. CONCLUSIONS AND FUTURE WORK

6.1 Conclusion

This thesis explains the affordable manufacturing process for creating nanofluidic channels on silicon, gold, and polymer. In an effort to stabilize the cost of manufacturing this nanofluidics, we have chosen several different materials and processes such as silicon, gold, and polymer. These nano channels have been integrated in between the micro channels from which the flow of fluid will be passed through and making it combination of MEMS/NEMS. The size of the nano channels which were formed were around 500 nm depth and 4 micrometers, which allows this device to separate those biomolecules from fluid and study their individual properties. Also, we successfully sealed the top surface of channels with PDMS bonding, which is one of the most cost-efficient ways of sealing the device. This fabrication process will have significant application in different industries of science and engineering.

This thesis first demonstrates the manufacturing process used in building micro channels with length, width, and depth. It has reservoirs to simplify the process of fluid flow at inlet and outlet of microchannel. Special care was taken in maintaining the space between the two micro channels by performing RIE, which ranges from 4-7 microns. Many papers have been published showing the individual work of manufacturing process for different materials. In our work, we developed micro channels on silicon wafer, and we used the same device for multiple applications by depositing the material on top of it, which has significantly reduced manufacturing time and directly reduces the cost associated in developing such devices for people who are in need of cheaper medical services. Micro channels were made of S-1813 photoresist of 10 micrometer in thickness, and around 200 nm of gold were deposited on the top of the silicon micro channel wafer.

A diamond tip was used for scratching the top of the silicon, but, as we know, this tip is a very expensive tool, which increases the cost of the device. To avoid such extra cost, we have utilized a tip made of carbide, and the cantilever is made of silicon to scratch the surfaces, such as gold and polymer, which are comparatively softer when compared to silicon. PDMS direct bonding technique was used to close this device from the top. SYLGARD-184 was cured to optimum temperatures and bonded to silicon. We believe that this research will not only contribute to the medical industry in building the biomolecule separation devices but also will be more affordable, which is very necessary for people who are in need of medical assistance.

6.2 Future Work

This thesis has explored several different manufacturing processes with the cost evaluation; there is a still hope of developing the technology to improve the control of nano scratching with more precision. Molecular dynamic simulation development is being developed using advanced algorithms that pre-determine the atom removal from the material. In the future, this technique will allow us to perform better nano scratching. The developed technique can be used for research purposes in research facilities, and there is great potential to develop more advanced techniques to implement this kind of fabrication in bulk production. The cost will be significantly reduced if we can develop such a process. There is also a good opportunity to integrate existing nano electronic system into this current devices for various other applications.

REFERENCES

REFERENCES

[1] A. T. Conlisk, "The debye-hückel approximation: Its use in describing electroosmotic flow in micro-and nanochannels," *Electrophoresis*, vol. 26, no. 10, pp. 1896–1912, 2005.

[2] J. O. Tegenfeldt, C. Prinz, H. Cao, R. L. Huang, R. H. Austin, S. Y. Chou, E. C. Cox, and J. C. Sturm, "Micro-and nanofluidics for dna analysis," *Analytical and bioanalytical chemistry*, vol. 378, no. 7, pp. 1678–1692, 2004.

[3] P. M. Sinha, G. Valco, S. Sharma, X. Liu, and M. Ferrari, "Nanoengineered device for drug delivery application," *Nanotechnology*, vol. 15, no. 10, p. S585, 2004.

[4] J. C. Eijkel and A. Van Den Berg, "Nanofluidics: what is it and what can we expect from it?" *Microfluidics and Nanofluidics*, vol. 1, no. 3, pp. 249–267, 2005.

[5] C. Rice and R. Whitehead, "Electrokinetic flow in a narrow cylindrical capillary," *The Journal of Physical Chemistry*, vol. 69, no. 11, pp. 4017–4024, 1965.

[6] H. Li and W. T. S. Huck, "Polymers in nanotechnology," *Current Opinion in Solid State and Materials Science*, vol. 6, no. 1, pp. 3–8, 2002.

[7] D. Mijatovic, J. Eijkel, and A. Van Den Berg, "Technologies for nanofluidic systems: top-down vs. bottom-upa review," *Lab on a Chip*, vol. 5, no. 5, pp. 492–500, 2005.

[8] R. Qiao and N. Aluru, "Ion concentrations and velocity profiles in nanochannel electroosmotic flows," *The Journal of chemical physics*, vol. 118, no. 10, pp. 4692–4701, 2003.

[9] S. C. Terry, J. H. Jerman, and J. B. Angell, "A gas chromatographic air analyzer fabricated on a silicon wafer," *Electron Devices, IEEE Transactions on*, vol. 26, no. 12, pp. 1880–1886, 1979.

[10] J. J. Kasianowicz, E. Brandin, D. Branton, and D. W. Deamer, "Characterization of individual polynucleotide molecules using a membrane channel," *Proceedings of the National Academy of Sciences*, vol. 93, no. 24, pp. 13 770–13 773, 1996.

[11] W. Lang, "Silicon microstructuring technology," *Materials Science and Engineering: R: Reports*, vol. 17, no. 1, pp. 1–55, 1996.

[12] G. J. Cheng, D. Pirzada, and P. Dutta, "Design and fabrication of a hybrid nanofluidic channel," *Journal of Micro/Nanolithography, MEMS, and MOEMS*, vol. 4, no. 1, pp. 013 009–013 009, 2005.

[13] M. Krishnan, I. Mönch, and P. Schwille, "Spontaneous stretching of dna in a two-dimensional nanoslit," *Nano letters*, vol. 7, no. 5, pp. 1270–1275, 2007.

[14] Y.-K. Lin and J.-N. Kuo, "Fabrication of sub-40 nm nanofluidic channels using thin glass-glass bonding," in *Nano/Micro Engineered and Molecular Systems (NEMS), 2011 IEEE International Conference on.* IEEE, 2011, pp. 351–354.

[15] Z.-Q. Wang, S. Tung, N.-D. Jiao, and Z.-L. Dong, "Nanochannels on silicon oxide surface fabricated by atomic force microscopy," in *Nano/Micro Engineered and Molecular Systems (NEMS), 2010 5th IEEE International Conference on.* IEEE, 2010, pp. 637–640.

[16] H. Cao, Z. Yu, J. Wang, J. O. Tegenfeldt, R. H. Austin, E. Chen, W. Wu, and S. Y. Chou, "Fabrication of 10 nm enclosed nanofluidic channels," *Applied physics letters*, vol. 81, no. 1, pp. 174–176, 2002.

[17] P. J. Kemery, J. K. Steehler, and P. W. Bohn, "Electric field mediated transport in nanometer diameter channels," *Langmuir*, vol. 14, no. 10, pp. 2884–2889, 1998.

[18] G. Karniadakis, A. Beskok, and N. Aluru, *Microflows and nanoflows: fundamentals and simulation.* Springer Science & Business Media, 2006, vol. 29.

[19] J. N. Israelachvili, *Intermolecular and surface forces: revised third edition.* Academic press, 2011.

[20] C. G. Y. Wu, S. Prakash and M. A. Shannon, "Solid/water interface charge density of surface functionalized materials studies by atomic force microscope," 2007.

[21] N. Petersen, J. Alarie, S. Jacobson, and J. Ramsey, "Polyelectrolyte transport in nanoconfined channels," in *Proc. 7th Int. Conf. Miniaturized Chem. Biochem. Anal. Syst*, 2003.

[22] S. Prakash, J. Yeom, N. Jin, I. Adesida, and M. Shannon, "Characterization of ionic transport at the nanoscale," *Proceedings of the Institution of Mechanical Engineers, Part N: Journal of Nanoengineering and Nanosystems*, vol. 220, no. 2, pp. 45–52, 2006.

[23] D. M. Cannon, T.-C. Kuo, P. W. Bohn, and J. V. Sweedler, "Nanocapillary array interconnects for gated analyte injections and electrophoretic separations in multilayer microfluidic architectures," *Analytical chemistry*, vol. 75, no. 10, pp. 2224–2230, 2003.

[24] C. Wei and T. Yih, "What is nanomedicine?" *Transfer*, vol. 3, p. A5, 2007.

[25] S. Tung, J.-W. Kim, A. Malshe, C. Lee, and R. Pooran, "A cellular motor driven microfluidic system," in *TRANSDUCERS, Solid-State Sensors, Actuators and Microsystems, 12th International Conference on, 2003*, vol. 1, June 2003, pp. 678–681 vol.1.

[26] N. L. Torcellini, Paul A. and R. Judkoff, "Consumptive water use for us power production," 2003.

[27] UNICEF and WHO, "Water for life: Making it happen," 2005.

[28] J. Han and H. G. Craighead, "Separation of long dna molecules in a microfabricated entropic trap array," *Science*, vol. 288, no. 5468, pp. 1026–1029, 2000. [Online]. Available: http://www.sciencemag.org/content/288/5468/1026.abstract

[29] H. T. H. et al, "Fabrication and interfacing of nanochannel devices for single-molecule studies," *Journal of Micromechanics and Microengineering*, vol. 19, no. 6, 2009.

[30] L. Guerin, M. Bossel, M. Demierre, S. Calmes, and P. Renaud, "Simple and low cost fabrication of embedded micro-channels by using a new thick-film photoplastic," in *Solid State Sensors and Actuators, 1997. TRANSDUCERS '97 Chicago., 1997 International Conference on*, vol. 2, Jun 1997, pp. 1419–1422 vol.2.

[31] M. LLC, *Cleanroom classification/particle count/FS209E/ISO TC209/*, (accessed 2014-01-11). [Online]. Available: http://www.cleanroom.byu.edu

[32] R. Darling, *Exposure and imaging*, (accessed 2014-05-10). [Online]. Available: https://washington.edu

[33] H. Sharifi and G. Gardner, *PLASMA RIE ETCHING FUNDAMNETALS AND APPLICATIONS*, (accessed 2013-05-10). [Online]. Available: https://nanohub.org

[34] R. Promyoo, H. El-Mounayri, and K. Varahramyan, "Afm-based nanoscratching: A 3d molecular dynamics simulation with experimental verification," in *ASME 2014 International Manufacturing Science and Engineering Conference collocated with the JSME 2014 International Conference on Materials and Processing and the 42nd North American Manufacturing Research Conference*. American Society of Mechanical Engineers, 2014, pp. V001T03A011–V001T03A011.

[35] G. Binnig, C. F. Quate, and C. Gerber, "Atomic force microscope," *Physical review letters*, vol. 56, no. 9, p. 930, 1986.

[36] R. Jagtap and A. Ambre, "Overview literature on atomic force microscopy (afm): Basics and its important applications for polymer characterization," *Indian Journal of Engineering and Materials Sciences*, vol. 13, no. 4, p. 368, 2006.

[37] N. Instruments, *Metal Carbide-coated AFM Probes*, (accessed 2013-09-15). [Online]. Available: https://nanoscience.com

[38] B. Lee, S. Seok, and K. Chun, "A study on wafer level vacuum packaging for mems devices," *Journal of micromechanics and microengineering*, vol. 13, no. 5, p. 663, 2003.

[39] B. A. Probes, *Diamond Tip p-3385*, (accessed 2014-01-24). [Online]. Available: https://brukerafmprobes.com

[40] D. C. Abeysinghe, S. Dasgupta, H. E. Jackson, and J. T. Boyd, "Novel mems pressure and temperature sensors fabricated on optical fibers," *Journal of micromechanics and microengineering*, vol. 12, no. 3, p. 229, 2002.

[41] Y.-Q. H. et al, "Experiments on the mechanical behavior of anodically bonded interlayer of pyrex glass/al/si," 2013.

[42] T. M. Lee, D. H. Lee, C. Y. Liaw, A. I. Lao, and I.-M. Hsing, "Detailed characterization of anodic bonding process between glass and thin-film coated silicon substrates," *Sensors and Actuators A: Physical*, vol. 86, no. 1, pp. 103–107, 2000.

[43] R.-H. I. of Technology, *Experimental Procedure for Anodic Bonding*, (accessed 2014-03-03). [Online]. Available: https://rose-hulman.edu

[44] J. Wei, H. Xie, M. Nai, C. Wong, and L. Lee, "Low temperature wafer anodic bonding," *Journal of Micromechanics and Microengineering*, vol. 13, no. 2, p. 217, 2003.

[45] S.-W. Choi, W.-B. Choi, Y.-H. Lee, B.-K. Ju, M.-Y. Sung, and B.-H. Kim, "The analysis of oxygen plasma pretreatment for improving anodic bonding," *Journal of the Electrochemical Society*, vol. 149, no. 1, pp. G8–G11, 2002.

[46] M. K. C. Bjorn Samel and G. Stemme, "The fabrication of microfluidic structures by means of full-wafer adhesive bonding using a poly(dimethylsiloxane) catalyst," *Micromech. Microeng*, vol. 17, no. 8, pp. 1710–1714, 2007.

[47] J. C. McDonald and G. M. Whitesides., "Poly(dimethylsiloxane) as a material for fabricating microfluidic devices," *Accounts of chemical Research*, vol. 35, no. 7, 2002.

[48] W. W. Y. Chow, K. F. Lei, G. Shi, W. J. Li, and Q. Huang, "Microfluidic channel fabrication by pdms-interface bonding," *Smart materials and structures*, vol. 15, no. 1, p. S112, 2006.

[49] M. A. Eddings, M. A. Johnson, and B. K. Gale, "Determining the optimal pdms–pdms bonding technique for microfluidic devices," *Journal of Micromechanics and Microengineering*, vol. 18, no. 6, p. 067001, 2008.

[50] L. Brown, T. Koerner, J. H. Horton, and R. D. Oleschuk, "Fabrication and characterization of poly (methylmethacrylate) microfluidic devices bonded using surface modifications and solvents," *Lab on a Chip*, vol. 6, no. 1, pp. 66–73, 2006.

[51] C.-W. Tsao and D. L. DeVoe, "Bonding of thermoplastic polymer microfluidics," *Microfluidics and Nanofluidics*, vol. 6, no. 1, pp. 1–16, 2009.

[52] Clariant, *AZ 1500 Photoresist-Photoresists*, (accessed 2014-04-04). [Online]. Available: https://photoresist.com